Biomass Conversion and Biorefinery (2026) 16:19
https://doi.org/10.1007/s13399-025-07017-2

ORIGINAL ARTICLE

Conversion of waste from the vegetable oil industry into efficient adsorbents for dye removal: thermo-chemical modification of hydrochar with green modifiers, adsorption kinetics and mechanisms

Aleksandra Petrovič[1] · Patricija Završki[1] · Muzafera Paljevac[1] · Sabina Vohl[1] · Lidija Čuček[1] · Marjana Simonič[1]

Received: 13 March 2025 / Revised: 23 October 2025 / Accepted: 27 October 2026

Abstract
The discharge of synthetic dyes into aquatic environments poses a significant environmental threat. Waste from the vegetable oil industry, such as hemp oil cake, offers a low-cost feedstock for the production of carbonaceous adsorbents for water purification due to its high carbon content and availability. In this study, hydrochars produced from hemp oil cake and cheese whey were thermo-chemically modified using natural vinegars and compared with conventional modifiers, then tested for adsorption of bromocresol green (BCG) and methylene blue (MB) dyes. According to FTIR, BET and SEM-EDS analyses, modifications with alcoholic and wine vinegar, acetic acid and KOH significantly altered the structural properties of the hydrochars, increasing the specific surface area from 1.60 to 234.35, 260.73, 71.32 and 582.84 m²/g, respectively. Among the acid-modified hydrochars, the hydrochar modified with alcoholic vinegar was the most effective, with an adsorption capacity of 15.45 mg/g for BCG and 62.16 mg/g for MB, as determined by Langmuir kinetic model, while the unmodified hydrochar had lower capacities. In comparison, the highest adsorption capacities for KOH-modified hydrochar were 640.15 mg/g for MB and 38.17 mg/g for BCG. Adsorption kinetics mostly followed a pseudo-second order model, indicating a combination of chemical and physical adsorption mechanisms driven byelectrostatic interactions, hydrogen bonding and π–π interactions. Isothermal kinetic modelling revealed heterogeneous adsorption behaviour, with the Redlich-Peterson and Freundlich models providing the best fit to the experimental data. The results emphasise the enhanced effectiveness of thermo-chemically modified hemp oil cake hydrochars for sustainable dye removal and water purification applications.

Keywords Hydrothermal carbonization · Hydrochar modification · Lignocellulosic biomass · Adsorption · Kinetics · Dyes

1 Introduction

Water pollution is a serious global environmental problem that strongly affects ecosystems, human health, and the economy [1]. The main sources of water pollution are industrial processes, which release harmful chemicals such as dyes and heavy metals, and agriculture, which uses fertilisers, pesticides, and other chemical substances [2]. The increasing discharge of synthetic dyes into aquatic environments poses a significant threat as these dyes are often toxic, carcinogenic, and resistant to biodegradation, making their removal from wastewater a critical environmental challenge [3]. Methylene blue (MB) and bromocresol green (BCG) are among the most widely used dyes in the textile and other industries, with MB also used in medicine [4]. Water contaminated with dyes such as MB and BCG is a significant environmental problem and poses several risks, as dyes impair water quality, increase biochemical and chemical oxygen demand, and hinder photosynthesis [5]. Dyes contain harmful chemicals such as sulphur, naphthol, and heavy metals that can accumulate in aquatic organisms and enter the food chain [6], leading to skin irritation and potentially cancer [7].

✉ Aleksandra Petrovič
aleksandra.petrovic@um.si

[1] Faculty of Chemistry and Chemical Engineering, University of Maribor, Smaetanova ul. 17, Maribor 2000, Slovenia

Published online: 06 January 2026

Numerous methods for dye removal have been developed, including physical (adsorption, coagulation, membrane filtration), chemical (electro-Fenton, photocatalysis, ozonation), and biological (enzymes, microbes, biosorption) approaches [8]. Conventional treatment methods such as membrane filtration are often ineffective in achieving complete removal of dyes and their toxic properties [6]. Therefore, various advanced methods for dye removal from wastewater have been explored, including advanced oxidation processes for the degradation of BCG and rhodamine B [9], chitosan-based hydrogels for adsorption of dyes and heavy metals [10], photocatalytic degradation of dyes using nano-sized metal oxides [4] and modified zeolites as catalysts [11]. In addition, adsorption using composites [12], as well as specific adsorbents such as metal-organic frameworks (MOFs) [13], and advanced nanomaterials such as azo-functionalised superparamagnetic iron oxide nanoparticles [14] and chitin nanofibers [15] have been investigated for the removal of specific dyes. Compared to the above-mentioned methods, adsorption has proven to be a superior method for the removal of dyes from wastewater due to its cost-effectiveness and environmental friendliness [16], with modified adsorbents being particularly promising because of their unique properties and high adsorption capacity [17]. Although adsorption is generally an effective method, challenges remain in developing novel materials for highly efficient dye removal in the practical application of adsorption technology for dye removal [18]. Recent research has mainly focused on developing novel adsorbents through functionalisation and modification methods to improve adsorption capacities [13], optimising the adsorption process to enhance the treatment of dye-contaminated wastewater, and understanding adsorption mechanisms [19].

Various types of adsorbents, including biosorbents and activated carbons prepared from biomass [20] and agro-industrial wastes [2], nanomaterials [21], and metal-organic frameworks [22], have been tested for their ability to remove dyes and other pollutants from water. The use of ion-exchange resins and functionalized silica as adsorbents is also known, but is limited by high production costs, regeneration difficulties, and environmental concerns related to their disposal [23]. Activated carbons derived from biochar or hydrochar, by contrast, have gained attention mainly due to their high adsorption efficiency, tunable surface properties [24], fast kinetics, low-cost production, and wide availability [8], and are therefore among the most commonly used adsorbents for dye removal. In particular, the hydrothermal valorization of waste biomass to hydrochar has proven to be a sustainable method for producing adsorbents, mainly due to the minimal energy consumption during production (the process takes place at low temperatures, between 180 and 250 °C) and the promising adsorption capacity of the resulting adsorbents [25].

Waste from the vegetable oil industry, such as shells and husks [26], oilseed cakes [27], and spent bleaching earth [28], has shown promising potential as natural adsorbents. These materials are rich in lignocellulosic content and possess functional groups (e.g., hydroxyl, carboxyl) that facilitate dye binding through various adsorption mechanisms [29]. Furthermore, modifications such as thermal treatment and acid or base treatment can significantly enhance their surface area and adsorption performance [30]. However, only a few studies have focused on the adsorption of dyes using residues from the vegetable oil industry and their biochars or hydrochars. For example, sunflower oil cake biochar obtained by pyrolysis [31] was tested alongside HTC-derived and NaOH-modified olive oil cake hydrochar for MB adsorption [32], but showed relatively low adsorption capacities. The composite prepared from kaolinite clay and moringa seed cake was successful in removing MB and acid orange-7 dyes from aqueous solutions [27]. Most recently, nanoparticle composites synthesised from hemp seeds, which can simultaneously remove chemical pollutants and inhibit microorganisms, have been used for the adsorption of lead, ibuprofen, and MB from aqueous solution, showing encouraging results [33]. These studies demonstrate the promising potential of vegetable oil industry residues and their derived biochars or composites as efficient, low-cost adsorbents for removing dyes and other contaminants from wastewater, while emphasizing the need for further research to optimize their modification and adsorption performance for practical large-scale applications.

To enhance the functionality of adsorbents, chemical modification has become an important topic in recent years. As the adsorption capacity of biochar is often relatively low, chemical modification has been introduced to improve its adsorption properties [17]. Various modification methods, including chemical and thermal treatments, mineral enrichment, and nanocomposite formation, can enhance the physicochemical properties and adsorption capacity of biochar [34]. Modified biochars demonstrate improved performance in pollutant removal and can also be used as soil conditioners, adsorbents, electrochemical materials, and catalysts [17]. Recent research has focused on using agricultural waste as feedstock for biochar production and exploring various modification methods, such as doping with Fe and N species, to increase its efficiency in removing pollutants from water and soil [35]. The choice of modification method depends on the target pollutants, environmental conditions, and remediation objectives. The most commonly used modifying reagents include strong acids (H_2SO_4, HCl, etc.) [36] and bases (NaOH, KOH, etc.) [26], while the use of natural reagents is rarely reported. In one of the earlier studies, the surface modification of wood biochar using natural coconut vinegar and its potential to remove aqueous calcium ions

in column and batch laboratory tests was investigated [37]. Some organic acids such as citric and acetic acid, have also been tested as green modifiers for biochar, with citric acid in particular improving MB adsorption efficiency [38].

In view of the above, the aim of this research was to produce hydrochar by hydrothermal carbonization and to improve its chemical properties and adsorption capacity through thermal and chemical modification using alternative natural chemical reagents. For the first time, hemp oil cake was used as a biomass source to produce hydrochar, as its adsorption capacity had not previously been investigated. The novelty of this work also lies in the introduction of alternative natural modifiers, specifically the residues from vinegar production, i.e. alcoholic vinegar and wine vinegar, which act as mild acids and influence the chemical properties of the adsorbents. Conventional modifiers, acetic acid and KOH, were also tested and compared as references. The modified hydrochars were chemically characterised, and the influence of the modification on the adsorption capacity for the dyes MB and BCG was investigated. To study the kinetics and sorption mechanism of the modified adsorbents, the data obtained were analysed using various kinetic models, and the adsorbents were additionally subjected to SEM-EDS and FTIR analyses.

2 Materials and methods

2.1 Preparation and modification of adsorbent

The adsorbent, hydrochar, was produced by hydrothermal carbonization (HTC) of hemp oil press cake (obtained after oil extraction from industrial hemp by a local vegetable oil producer) and cheese whey (which acted as the liquid reaction medium) at 250 °C and a reaction time of 5 h. The detailed properties of the feedstocks and the preparation procedure of feedstocks are described in a previous article published by the authors [39]. The reaction mixture contained 30 g of oil cake and 180 g of cheese whey (mass ratio 1:6). The reaction was conducted in a stainless-steel autoclave reactor, heated in an oven at a heating rate of 4 °C/min. The produced hydrochar was separated from the process liquid by vacuum filtration, washed three times with distilled water, and dried at 105 °C to constant weight.

The hydrochar produced using the HTC method (sample "H") was chemically modified with four different chemical reagents (Table 1). Two conventional modifiers, potassium hydroxide (KOH) and acetic acid, were tested. In addition, two alternative natural reagents were used as green modifiers: 9% alcoholic vinegar and 6.6% wine vinegar obtained by natural acidification. Alcoholic vinegar and wine vinegar were selected for their natural acetic acid content and the presence of organic esters and phenolic compounds from fermentation, which can introduce oxygenated functional groups to the hydrochar surface. Differences in their chemical composition (in organic acids and other components) were expected to influence surface oxidation and polarity differently, enabling a comparative evaluation of two "green" acidic modifiers.

The hydrochar was mixed with the modifier at a ratio of 1:2. The chemical modification was conducted for 16 h. The mixture was then dried at 105 °C. Subsequently, thermal modification (pyrolysis) was carried out in a nitrogen atmosphere at 800 °C for 1 h. After thermal treatment, the KOH-modified hydrochar was washed with 0.1 M HCl, followed by distilled water, and then dried at 105 °C. For comparison, one hydrochar sample was only thermally treated at 800 °C for 1 h in a nitrogen atmosphere, without prior chemical modification. The activated hydrochars were stored in a desiccator until further characterization or adsorption experiments. The samples were labelled as shown in Table 1.

2.2 Physico-chemical characterization of the adsorbents

The adsorbents underwent elemental and proximate analyses, including determination of moisture, dry matter, ash content (800 °C, 4 h), and volatile matter content (900 °C, 1 h). The surface charge (zeta potential) of the adsorbents was analysed in distilled water using the Zetasizer Nano ZS (Malvern), a system for laser measurement of particle size and zeta potential. The point of zero charge (pH_{PZC}) of the adsorbents was determined as follows: 20 mg of adsorbent was mixed with 0.01 M NaCl solutions of varying pH,

Table 1 Chemical modifiers and modification conditions

Sample	Chemical reagent	Time of chemical modification (h)	Ratio hydrochar/reagent	Thermal modification (temperature, time)
H	/	/	/	/
H-800	/	/	/	800 °C, 1 h
H-AV-800	9% alcoholic vinegar	16	1:2	800 °C, 1 h
H-WV-800	6.6% wine vinegar	16	1:2	800 °C, 1 h
H-AA-800	18% acetic acid	16	1:2	800 °C, 1 h
H-KOH-800	60% KOH	16	1:2	800 °C, 1 h

adjusted with 0.1 M HCl or NaOH. The samples were then placed on a shaker (150 rpm) for 24 h, after which the final pH of the solutions was measured. Graphs of △pH values were plotted against initial pH values, with the intercept indicating the isoelectric point. The surface area, pore size, and pore volume were determined using the Micromeritics Tristar II 3020 Porosimeter (USA) with the Brunauer-Emmett-Teller (BET) method. The adsorbents were also examined by high-resolution scanning electron microscopy (SEM-EDS) using the JSM IT-800SHL microscope and the AZtec Live AUTO UltimMax 100 EDX spectrophotometer. Fourier transform infrared spectroscopy (FTIR) with the KBr pellet method was used to characterize the functional groups on the surface of the adsorbents. Measurements were performed with a Shimadzu IRAffinity-1 S spectrophotometer.

2.3 Batch adsorption experiments

Batch adsorption experiments were conducted with MB and BCG dyes using unmodified, thermally modified and thermo-chemically modified hydrochars (see Table 1). For each experiment, 50 ml of dye solution at a specific concentration was added to an Erlenmeyer flask containing the adsorbent and shaken at 200 rpm at a constant room temperature (23 ± 1 °C). The pH and contact time were adjusted separately for each of the experiments. The pH was adjusted with 1 M HCl or 1 M NaOH solution. The adsorption experiments were carried out in parallel. Samples for analysis of MB and BCG concentrations were taken at different time intervals, filtered, and diluted accordingly with distilled water. The dye concentration in the solution was determined spectrophotometrically using a Varian Cary 50 UV–VIS spectrophotometer at a wavelength of 665 nm for MB dye and 424 nm for BCG dye.

2.3.1 Investigation of adsorption kinetics and the effects of hydrochar modification on adsorption

The kinetics of adsorption and the effect of hydrochar modification on the adsorption of the selected dyes were investigated at an initial concentration of 50 mg/L for MB dye (contact time 168 h, pH 7) and at an initial concentration of 25 mg/L for BCG dye (contact time 96 h, pH 5). A mass of 0.05 g adsorbent was added to 50 ml of dye solution.

2.3.2 Study of the influence of pH on dye adsorption

The effect of pH on adsorption performance was investigated for the modified adsorbents that exhibited the highest adsorption efficiency in preliminary studies, namely samples H-AV-800 and H-KOH-800. For comparison, the test was also conducted with unmodified hydrochar (sample H) and pyrolyzed hydrochar (H-800). The adsorption of MB was examined at an initial dye concentration of 50 mg/L, using 0.05 g of adsorbent, and at pH values of 4, 6, 8, and 10. This pH range was selected to cover the environmentally relevant values typically found in natural and industrial wastewater systems, and to ensure the chemical stability of both dyes and hydrochars without causing chemical degradation of either the adsorbent or the adsorbate.

An exception was the sample H-KOH-800, which had an initial concentration of 100 mg/L and an adsorbent mass of 0.01 g. The adsorption of BCG was investigated at pH values of 4, 5, 6, 7 and 8 with an initial dye concentration of 25 mg/L and an adsorbent mass of 0.05 g, except for the sample H-KOH-800, which had a concentration of 50 mg/L and an adsorbent mass of 0.02 g. The reaction time for MB adsorption was 168 h, and for BCG, 96 h. Different dye concentrations and adsorbent doses were selected to ensure that the adsorption process reached measurable equilibrium conditions for each sample. Besides, dyes with different chemical compositions have different adsorption mechanisms. Preliminary experiments also showed that the adsorbents have quite different adsorption capacities; therefore, the experimental conditions were adjusted accordingly. Specifically, the KOH-modified hydrochar exhibited significantly higher adsorption capacity and faster adsorption kinetics compared to the other samples. Consequently, lower adsorbent masses and higher initial dye concentrations were used to prevent complete dye removal within a few minutes and to maintain sufficient dye concentration for accurate modelling. This adjustment ensured comparable data reliability and avoided analytical saturation.

2.3.3 Studying the effect of dye concentration on adsorption performance

Isothermal adsorption experiments were conducted to assess the adsorption of MB dye within a concentration range of 5–300 mg/L, at pH value 8 and a reaction time of 96 h. The adsorbent mass was 0.01 g for sample H-KOH-800, 0.05 g for samples H and H-AV-800, and 0.1 g for sample H-800. Experiments with BCG were carried out using a concentration range of 5–75 mg/L, at pH value 5 and a reaction time of 96 h. The sample mass was 0.02 g for H-KOH-800, 0.04 g for H-AV-800, and 0.1 g for samples H and H-800. The volume of the dye solution was the same as in previous experiments.

2.3.4 Equations and isotherm kinetic models

The adsorption capacity of modified and unmodified adsorbents was calculated using Eq. 1 [40]:

$$q_t = \frac{(c_0 - c_t) * V}{m} \quad (1)$$

where q_t is the adsorption capacity in mg/g of the adsorbent, c_0 (mg/L) is the initial concentration of the dye, c_t (mg/L) is the concentration at time t, V(L) is the volume of the dye solution and m (g) is the amount of adsorbent.

To study the kinetics of MB and BCG adsorption, the pseudo-second order (Eq. 2) and pseudo-first order (Eq. 4) kinetic models were applied [41]. The models were verified for unmodified and modified hydrochars at only one concentration to study the influence of thermo-chemical modification on the adsorption kinetics. The pseudo-second order model is described by the following equation:

$$\frac{t}{q_t} = \frac{t}{q_e} + \frac{1}{k_2 \cdot q_e^2} \quad (2)$$

where k_2 represents the pseudo-second order rate constant [g/(mg·min)] and q_e the adsorption capacity at equilibrium (mg/g).

The equation for the pseudo-first order model can be written as:

$$\ln(q_e - q_t) = \ln q_e - k_1 \quad (3)$$

t

where k_1 is the pseudo-first order rate constant (min^{-1}).

The removal efficiency, $E(\%)$, was calculated as follows (Eq. 4):

$$E(\%) = \frac{(c_0 - c_t)}{c_0} * 100 \quad (4)$$

The Langmuir, Freundlich [42], Dubinin-Radushkevich [41], Toth and Redlich-Peterson [43] isotherm models, as expressed by the equations in Table A.1 of the Supplementary material, were fitted to the experimental data for MB and BCG adsorption using Matlab software.

3 Results and discussion

3.1 The influence of modification on the properties of adsorbents

Thermo-chemical modification (treatment temperature, duration, chemical reagent, its concentration, and duration of treatment) highly affect the structure and adsorption performance of hydrochar. Higher temperatures promote pore development and the volatilization of oxygenated groups [44], while the type of reagent (acid or base) determines surface functionality, particularly surface area, and also influences pore size and volume [45]. From this perspective, the physico-chemical and surface properties of the prepared adsorbents are discussed in the following sections.

3.1.1 Physico-chemical properties

The physico-chemical properties of the unmodified and thermo-chemically modified hydrochars are presented in Table 2. The unmodified hydrochar was rich in volatiles and contained little ash, whereas the modified samples, due to chemical and thermal treatment, exhibited the opposite characteristics. Changes in ash content also affect other hydrochar properties, such as surface area, pore volume, and sorption performance [42]. Several differences can be observed between the samples treated with acidic reagents (both vinegar and acetic acid) and those treated with the basic reagent, KOH, in terms of proximate and ultimate analysis, particularly in nitrogen (N) and oxygen (O) content, although the carbon (C) content was relatively similar. The KOH treatment contributes to the release of N from the hydrochar and the retention of O. Modification significantly increased the C content, especially in the sample subjected solely to thermal treatment (sample H-800). The samples treated with natural vinegars exhibited similar properties. According to the Van Krevelen diagram, the H/C and O/C ratios of the hydrochar decreased after thermo-chemical

Table 2 Results of the characterization of the adsorbents

Sample		H	H-800	H-AV-800	H-WV-800	H-AA-800	H-KOH-800
Volatile matter (wt%)		67.29	41.09	46.27	46.32	51.87	52.59
Ash content (wt%)		7.12	19.67	20.76	18.96	20.34	22.07
Ultimate analysis (wt%)	Carbon	62.39	72.35	66.41	69.68	66.25	65.86
	Hydrogen	7.02	1.89	4.62	4.17	4.42	4.31
	Nitrogen	6.32	4.28	3.21	3.31	3.14	1.71
	Sulphur	2.13	0.08	3.83	3.36	3.62	2.94
	Oxygen	15.02	1.73	1.17	0.52	2.23	3.11
Specific surface area (m^2/g)		1.60	15.57	234.35	260.73	71.32	582.84
Pore size (nm)		8.96	7.43	17.25	3.67	2.54	5.45
Volume of pores (cm^3/g)		0.0033	0.0086	0.1067	0.1308	0.0273	0.3164
Zeta potential (mV)		−27.3	−15.7	−29.8	−24.6	−17.3	−19.3
pH_{PZC}		6.51	7.76	7.34	7.40	6.05	9.58

modification (Fig. A.1a, Supplementary material). Hydrochar exposed only to pyrolysis at 800 °C showed the lowest H/C ratio among all samples, due to a significant decrease in H and an increase in C content. Regarding chemical treatment, vinegar and acetic acid have a stronger effect on the O/C ratio than KOH. In contrast, the H/C ratios were relatively similar for all chemically modified samples, with only minor differences. However, as natural vinegars were used as modifiers, the natural variability in their chemical composition (e.g., batch differences, source) might affect modification and the chemical and surface properties of the hydrochar. It should be noted, however, that both vinegars were obtained from a single local producer and the acetic acid content is always of the same concentration.

Chemical modification with acids or bases resulted in various chemical and structural changes in the hydrochars, including the introduction of new functional groups on the surface and the removal of impurities such as heavy metals [46]. During thermal treatment (pyrolysis at 800 °C), stable volatile components that did not volatilise during the HTC treatment were released. For example, oxygen-containing functional groups decompose to CO_2 or CO [47]. Similar chemical changes through chemical modification have also been observed in the modification of char with tartaric acid, acetic acid, and citric acid [48] or with KOH [49]. The reaction mechanism of chemical modification with KOH and its effects on adsorption were described in detail by Mamaní et al. [50] and involve the reaction of potassium with the carbonaceous components, forming a porous structure due to physical activation at high temperatures. KOH thus introduces microporosity and OH groups, whereas vinegars based on acetic acid generate carboxyl and carbonyl functionalities, improving electrostatic and π–π interactions with dye molecules. The reaction mechanism of acidic activation with organic acids was briefly explained by Lonappan et al. [51] and includes the functionalisation of the biochar with acidic functional groups such as COOH.

3.1.2 Surface properties

Parameters such as specific surface area, volume and pore size provide crucial information about the performance of adsorbents in the sorption of various pollutants and are considered the most important physical properties affecting adsorption capacity [52]. After thermo-chemical modification of the hydrochar, the specific surface area of the adsorbents increased. Sample H-KOH-800 had the highest specific surface area (582.84 m^2/g), with values decreasing in the following order: H-KOH-800 > H-WV-800 > H-AV-800 > H-AA-800 > H-800 > H. KOH has also proved to be an effective activator in previous studies, contributing significantly to the improvement of the porosity and surface area of the biochar [26]. KOH activation induces in-situ reactions between potassium compounds and carbon at elevated temperatures (800 °C), producing gaseous species (K_2CO_3, CO, CO_2) that etch the carbon matrix and create micropores [50]. In contrast, acid modifiers (vinegars, acetic acid) mainly cause surface oxidation and partial removal of minerals but do not significantly expand the pore network [36]. Therefore, the samples modified with natural vinegars exhibited about half the surface area of those samples modified with KOH, with sample H-WV-800 showing the best results among all acid modifiers. Interestingly, sample H-AV-800 exhibited a significantly larger pore size than the other samples, while the unmodified hydrochar (sample H) had the lowest pore volume. Knowing the pore size and its distribution is important because biochar with small pores cannot adsorb dyes composed of large molecules [53]. Chemical or thermal modification of adsorbents can have very different effects on their surface properties. Treatment with acids often leads to a slight reduction in surface area, while treatment with bases increases the surface area and introduces oxygen-containing functional groups [46]. Treatment with acids can also result in the loss of micropores, as micropores collapse with increasing amounts of acid [48]. This likely occurred during modification with acetic acid (sample H-AA-800), as 18% acetic acid is a stronger reagent than vinegar due to its higher acetic acid content.

FTIR analysis of the adsorbents (Fig. A.1b, Supplementary material) shows that the modified hydrochar contains distinctly different functional groups on the surface, including hydroxyl, carbonyl, carboxylate, and others, confirming that the modification has significantly altered the chemical composition of the hydrochar and that the presence of polar acidic groups enhances ion exchange and adsorption of cations. The spectrum of the unmodified hydrochar (sample H) shows significant peaks between 3600–2800 cm^{-1}, indicating the presence of O–H, N–H, and C–H bonds, while small peaks in the 1000–1800 cm^{-1} range correspond to C–N, C = C and C = O bonds. The peaks in the 650–850 cm^{-1} range can be attributed to aromatic structures [54]. The HTC process produces carbon-rich materials, which explains the presence of these functional groups on the hydrochar surface. During further thermos-chemical treatment of the hydrochar, some functional groups were removed and others introduced, altering the chemical composition and the FTIR spectrum. Sample H-800, which underwent only thermal pyrolysis treatment, is clearly different from the chemically treated samples as the intensity of its peaks was much lower, indicating that fewer functional groups are available for pollutant adsorption. The KOH-treated sample exhibited a broad peak for OH and C = O groups, while the samples treated with vinegars showed pronounced peaks for C–O (1150–1050 cm^{-1}) bonds and OH groups.

A peak for C = O bonds was also observed in the chemically modified samples, whereas the peaks for C–H bonds disappeared. Sample H-WV-800 showed similar characteristics to samples H-AV-800 and H-AA-800, as all were treated with acid-based reagents. KOH treatment therefore intensified the –OH and C = O bands, indicating hydroxylation and the formation of active sites for electrostatic and hydrogen-bond interactions with cationic MB. Vinegar and acetic acid modifications enhanced the C = O and –COOH bands, increasing polarity and adsorption of MB through electrostatic attraction and of BCG via hydrogen bonding and π–π interactions. The reduced C–H and aromatic C = C bands confirm surface oxidation and structural ordering favourable for dye binding. Similar changes in the surface chemical properties of adsorbents due to modification have been reported in other studies, for example after alkali treatment of biochar with KOH [55] or acidic treatment with nitric, sulphuric or hydrochloric acid [36].

The zeta potential of adsorbents, which reflects the electrical potential, i.e. the charge on the surface of a particle in a colloidal suspension resulting from the ionization of chemical groups, increased in the following order: H-AV-800 < H < H-WV-800 < H-KOH-800 < H-AA-800 < H-800. As the modified adsorbents in this study exhibited a negative zeta potential, they primarily promoted the adsorption of the cationic dye. The zeta potential strongly influences the adsorption process, although the surface charge of the functional groups on the adsorbent and the degree of ionization of the adsorbate are strongly affected by the pH of the solution [53]. In addition, other adsorption mechanisms (e.g. π-π interactions, hydrogen bonding) also influence the adsorption process and should be considered for each system. The pH value at which the surface charge is electrically neutral is referred to as the point of zero charge (pH_{PZC}). Below this point, the surface of the biochar is positively charged due to protonation of the surface functional groups, which promotes the adsorption of anionic dyes and inhibits the uptake of cationic dyes [56]. The unmodified hydrochar (H) exhibited an isoelectric point pH_{PZC} of 6.51 (Table 2), indicating a nearly neutral surface. After pyrolysis at 800 °C, the pH_{PZC} increased to 7.76, reflecting the partial removal of acidic oxygenated groups and the formation of more basic surface sites. Hydrochars modified with natural vinegars (H-AV-800 = 7.34, H-WV-800 = 7.40) retained slightly lower pH_{PZC} values compared to the thermally treated sample alone, suggesting the presence of carboxylic and carbonyl groups introduced by organic acids and reflecting a balance between mild oxidation and structural aromatization. In contrast, acidic modification with acetic acid (H-AA-800) decreased the pH_pzc to 6.05, confirming enhanced surface acidity, while alkaline activation with KOH (H-KOH-800) markedly increased it to 9.58, due to the introduction of oxygenated basic functional groups ($–OH^-$ and $–O^-$) [27]. These differences in surface charge behavior explain the adsorption trends observed for the dyes: cationic MB is preferentially adsorbed at $pH > pH_{PZC}$, where the adsorbent surface becomes negatively charged due to deprotonation of surface groups, resulting in electrostatic attraction between the negatively charged surface and the cationic dyes, generally improving adsorption [57], whereas anionic BCG adsorption is favored at $pH < pH_{PZC}$, when the surface is protonated and positively charged [31].

3.2 The results of adsorption studies

3.2.1 The influence of modification on adsorption kinetics

Figure 1 presents a comparison of the adsorption capacity and efficiency of unmodified and modified adsorbents for the adsorption of MB and BCG. The lowest adsorption capacity for the MB dye (3.25 mg/g) was observed for hydrochar H-800, subjected only to thermal treatment (Fig. 1a). Its adsorption capacity was even lower than that of unmodified hydrochar (17.11 mg/g). Among the vinegar-treated samples, the one treated with alcoholic vinegar (H-AV-800) showed the highest adsorption capacity (42.55 mg/g) and efficiency (81.91%), outperforming the sample treated with wine vinegar (H-WV-800, 29.42 mg/g). Wine vinegar treatment may have contributed to increased surface polarity or the introduction of carboxyl groups, which are beneficial for MB adsorption, although not as effective as alcohol vinegar modification. The sample treated with pure 18% acetic acid showed a decrease in adsorption performance compared to the vinegar-treated and unmodified hydrochar, probably due to acidification of the adsorbent surface, which could block active sites or reduce surface area, limiting the interaction between dye molecules and the adsorbent [36]. To better evaluate the performance of modified biochar, an additional experiment was conducted with KOH-modified hydrochar, as alkali-treated biochar is known for its large surface area and high adsorption capacity. The H-KOH-800 sample completely removed the MB dye from the water and had the highest adsorption capacity (52.15 mg/g) of all the samples tested.

The adsorption of BCG (Fig. 1b) was less efficient, with significantly lower adsorption capacities. The capacities followed the same order as those for the MB dye: sample H-KOH-800 had the highest capacity (29.31 mg/g), followed by samples H-AV-800, H-WW-800, H, H-800, and sample H-AA-800 with the lowest capacity (4.21 mg/g). The highest efficiencies were therefore observed for samples H-KOH-800 (99.27%) and H-AV-800 (48.39%). KOH activation proved to be the most promising method for increasing the adsorption capacity of the adsorbent. This is

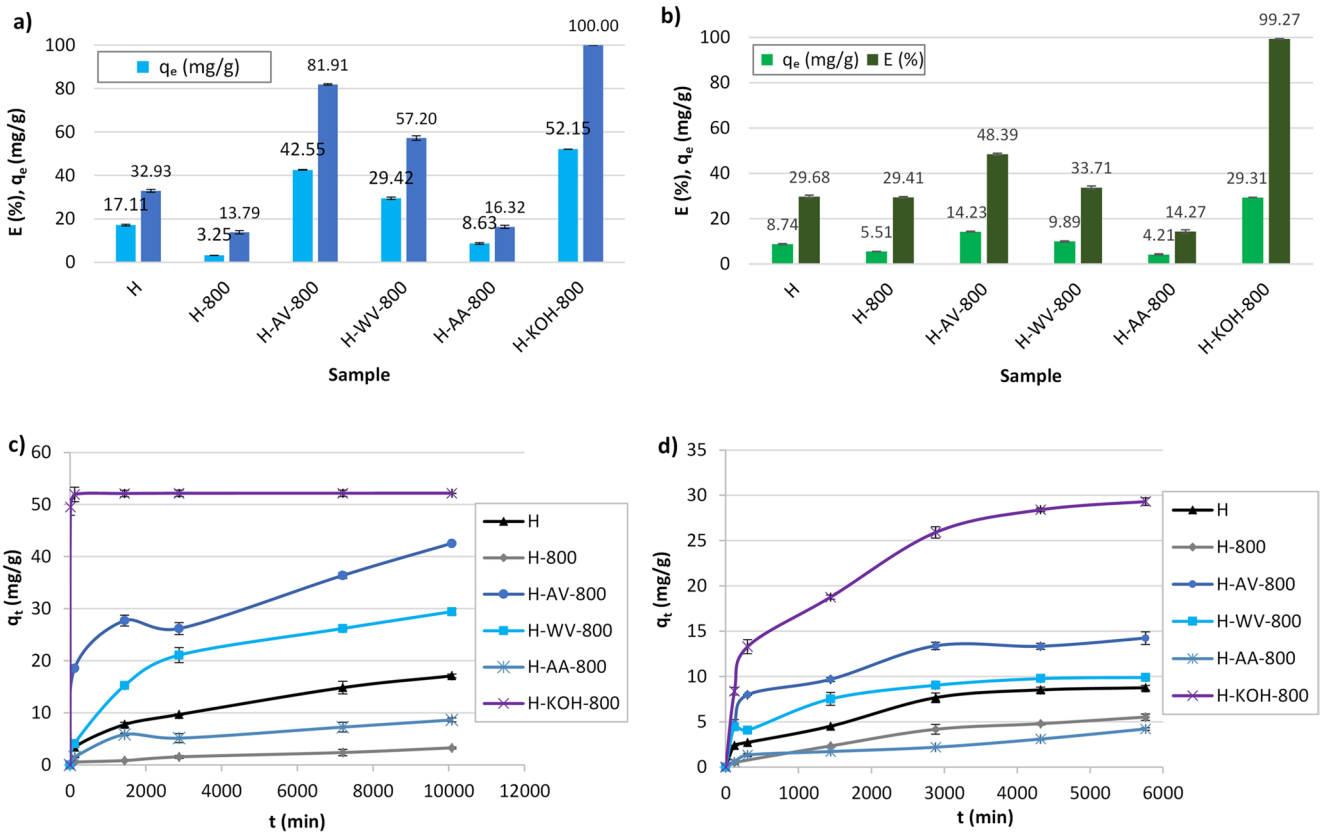

Fig. 1 Adsorption capacity and efficiency (**a**, **b**), and adsorption kinetics (**c**, **d**) for the adsorption of MB (graphs on the left) and BCG (graphs on the right) using unmodified and modified hydrochars (initial dye concentration: MB 50 mg/L, BCG 25 mg/L)

due to the increased porosity and the introduction of OH functional groups, which improve the interaction between the adsorbent and the adsorbate molecules, i.e. the dye [58]. Modification with alcohol vinegar showed greater potential than that with wine vinegar, while treatment with acetic acid appears to impair adsorption performance. Therefore, of the samples treated with acidic reagents, only sample H-AV-800 was used for further adsorption studies.

Contact time between the adsorbent and the dye solution (Fig. 1c, d) had a major influence on adsorption capacity, although most of the dye was adsorbed in less than 24 h. Slight differences were observed between the samples, indicating that the optimal contact time depends on the type of adsorbent and its modification. Adsorption of MB with the adsorbent H-KOH-800 occurred in less than 10 min, indicating extremely rapid adsorption of this dye. The literature review shows that contact time is one of the most important factors affecting adsorption performance, as it also influences the adsorption of dyes such as acid orange [27], as well as the adsorption of other pollutants [33]. In real systems, adsorption performance can also be affected by several other factors, as water may be contaminated with multiple dyes and other types of pollutants. For example, in a binary system, MB and BCG would likely compete for the same active sites, since both interact with oxygenated and aromatic functional groups on the hydrochar surface. Due to its smaller molecular size, cationic charge, and higher affinity for negatively charged sites, MB would be preferentially adsorbed, while BCG uptake would be significantly reduced. Such competitive effects could limit adsorption capacity under real wastewater conditions, which must be considered in process design.

MB and BCG adsorption generally followed the pseudo-second order kinetic model for the majority of adsorbents tested (Fig. 2), except for few samples. The calculated kinetic constants for the pseudo-second order and pseudo-first order kinetic models for each sample are listed in Table 3.

The kinetic constant k_2 of the pseudo-second order model was within the same range for most samples, although sample H-KOH-800 had a slightly higher value for MB adsorption. The correlation coefficients for the pseudo-second order model for MB adsorption were above 0.95, except for sample H-800 (R^2 = 0.82), while the values for BCG adsorption ranged from 0.84 to 0.99. The theoretical adsorption capacities of the second-order model mostly agree with the experimentally determined values. On the other hand, R^2 values for samples H-800 (for MB), H-800 (for BCG) and

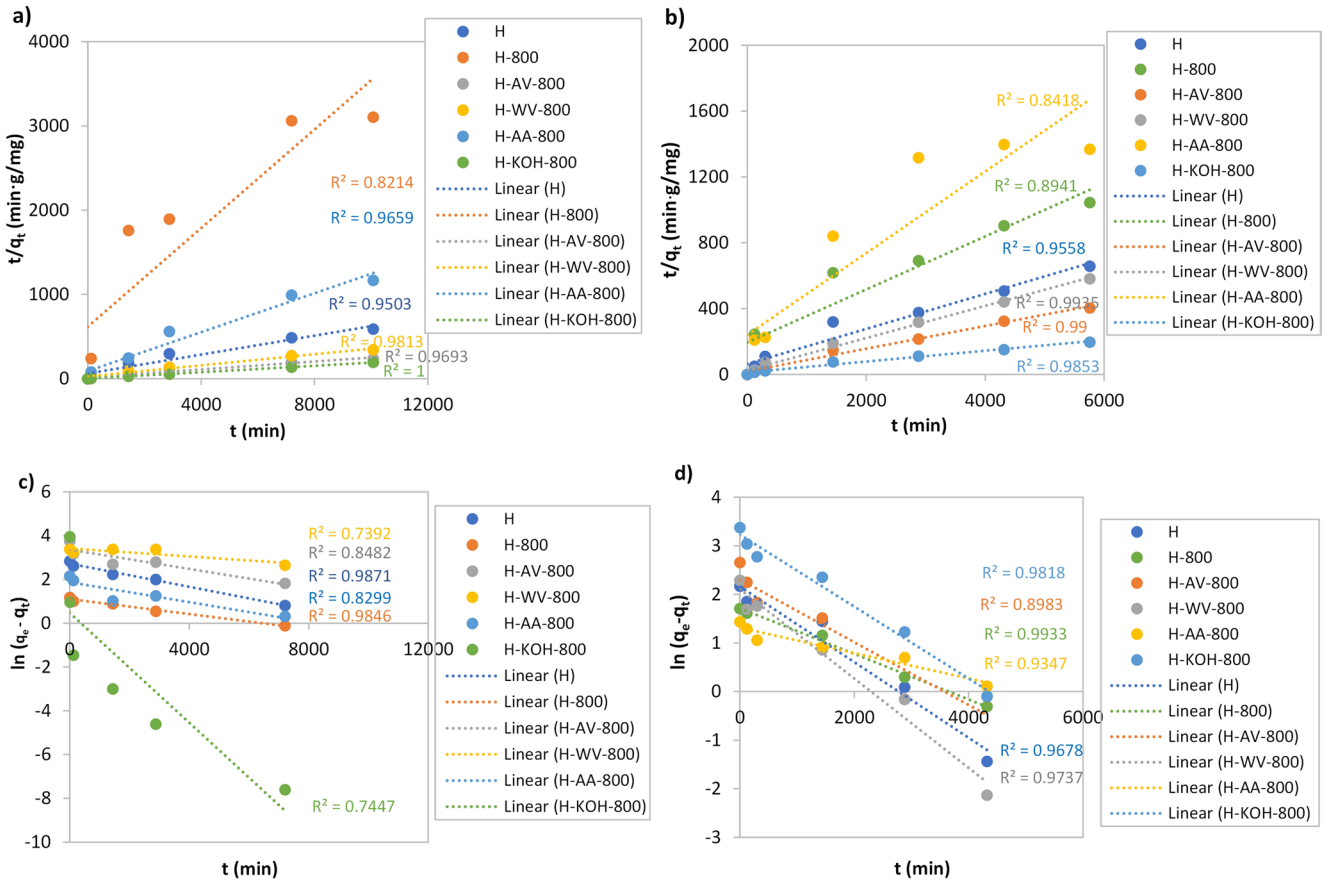

Fig. 2 **a**, **b**) Pseudo-second order kinetic model fitting and **c**, **d**) pseudo-first order kinetic model fitting for the adsorption of MB (graphs on the left) and BCG (graphs on the right) on unmodified and modified hydrochars (initial dye concentration: MB 50 mg/L, BCG 25 mg/L)

H-AA-800 (for BCG) are much higher for the pseudo-first order model than for the pseudo-second order model, indicating that these samples followed pseudo-first order kinetics rather than pseudo-second order kinetics. According to Tu et al. [26], the good agreement of experimental data with the pseudo-second order kinetic model indicates that chemisorption mechanisms predominate, whereas the pseudo-first order model is mainly characteristic of physisorption mechanisms. For methylene blue, adsorption likely involves electrostatic attraction between negatively charged surface groups (–COO^-, –OH^-) and cationic MB^+, hydrogen bonding between amine groups from MB and carboxyl/hydroxyl groups from hydrochar, and π–π interactions between the aromatic rings of MB and the graphitic domains of hydrochar. For BCG, electrostatic attraction predominates, especially at low pH due to protonated adsorbent surfaces.

3.2.2 The influence of pH value on adsorption performance

The pH of the solution significantly affects the adsorption of dye molecules, the zeta potential, and the surface charge properties of the adsorbent. It also influences the solubility of the adsorbates, as their molecular or ionic forms change in the solution [56]. The results of experiments investigating the effect of solution pH on the adsorption of MB and BCG, conducted with samples H, H-800, H-AV-800, and H-KOH-800, are presented in Fig. 3. The samples exhibited markedly different behaviour depending on the type of dye used. The equilibrium adsorption capacity (q_e) of unmodified hydrochar increased with rising pH when exposed to MB dye, whereas for BCG, the values initially increased and then fluctuated. For BCG dye, a general decrease in adsorption capacity with increasing pH was observed for the modified samples, with the most pronounced decrease at the highest pH values, particularly for sample H-KOH-800. On the other hand, a slight increase in adsorption capacity between pH 7 and 8 for H-800 may be attributed to secondary electrostatic and hydrogen bonding interactions that become more favorable in near-neutral to mildly alkaline environments. At alkaline pH, partial deprotonation of hydroxyl and carboxyl groups on the hydrochar surface occurs, but the overall surface charge remains only moderately negative, which still allows partial interaction with the negatively charged BCG molecules through hydrogen

Table 3 The kinetic constants of the pseudo-second and pseudo-first order kinetic models calculated for the adsorption of MB and BCG by the tested adsorbents (modified and unmodified hydrochars)

Dye	Parameter	Sample					
		H	H-800	H-AV-800	H-WV-800	H-AA-800	H-KOH-800
Pseudo-second order kinetic model							
MB adsorption	$q_{e,\,exp.}$ (mg/g)	17.11	3.25	42.55	29.42	8.63	52.15
	Slope	0.06	0.29	0.02	0.03	0.12	0.02
	Intercept	61.82	617.18	14.66	27.87	88.57	0.01
	R^2	0.95	0.82	0.97	0.98	0.97	1.00
	k_2 [g/(mg·min)]	5.5×10^{-05}	1.5×10^{-04}	3.8×10^{-05}	4.2×10^{-05}	1.5×10^{-04}	7.4×10^{-02}
	$q_{e,\,theor.}$ (mg/g)	17.76	3.42	42.19	30.58	8.64	52.08
BCG adsorption	$q_{e,\,exp.}$ (mg/g)	8.74	5.51	14.23	9.89	4.21	29.31
	Slope	0.11	0.16	0.07	0.10	0.25	0.03
	Intercept	42.18	194.91	19.16	26.84	240.91	12.52
	R^2	0.99	0.89	0.99	0.99	0.84	0.99
	k_2 [g/(mg·min)]	3.1×10^{-04}	1.7×10^{-04}	2.6×10^{-04}	3.8×10^{-04}	2.4×10^{-04}	9.3×10^{-05}
	$q_{e,\,theor.}$ (mg/g)	9.19	6.21	14.49	10.25	4.03	30.49
Pseudo-first order kinetic model							
MB adsorption	Slope	−0.0003	−0.0002	−0.0002	−0.00009	−0.0002	−0.0015
	Intercept	2.7189	1.1001	3.3603	3.4193	1.8740	0.4809
	R^2	0.9871	0.9846	0.8482	0.7392	0.8299	0.7447
	k_1 (min^{-1})	3.0×10^{-04}	2.0×10^{-04}	2.0×10^{-04}	9.0×10^{-05}	2.0×10^{-04}	1.5×10^{-03}
	$q_{e,\,theor.}$ (mg/g)	15.16	3.00	28.79	30.54	6.51	1.62
BCG adsorption	Slope	−0.0008	−0.0005	−0.0006	−0.0009	−0.0009	−0.0007
	Intercept	2.1621	1.717	2.3064	2.109	1.3124	3.2313
	R^2	0.9678	0.9933	0.8983	0.9737	0.9347	0.9818
	k_1 (min^{-1})	8.0×10^{-04}	5.0×10^{-04}	6.0×10^{-04}	9.0×10^{-04}	9.0×10^{-04}	7.0×10^{-04}
	$q_{e,\,theor.}$ (mg/g)	8.69	5.57	10.04	8.24	3.71	25.30

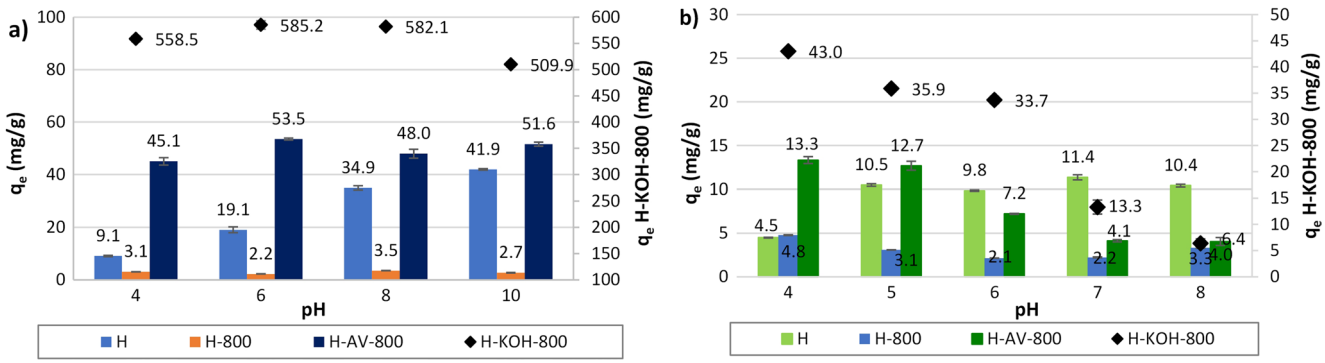

Fig. 3 Adsorption capacity of selected unmodified and modified hydrochars as a function of pH for the adsorption of: (**a**) MB and (**b**) BCG dye

bonding and π–π interactions. Moreover, changes in the ionization state of the BCG dye near its pKa result in a mixture of molecular species with different affinities, which can impact adsorption at higher pH values.

The optimum pH for BCG adsorption by modified hydrochars was around 4, and for unmodified hydrochar between 5 and 7. The KOH-modified sample showed the largest decrease in adsorption capacity among all samples.

Regarding the adsorption of MB, the changes in adsorption capacity due to pH variations were smaller than those observed for the adsorption of BCG. Samples H, H-AV-800, and H-KOH-800 showed a slight increase in adsorption capacity as the pH increased from 4 to 6, whereas sample H-800 showed a decrease. The adsorption of MB on unmodified hydrochar was most sensitive to pH changes, with the optimum pH for MB adsorption by this sample being between 8 and 10. Modified samples exhibited their best performance in the pH range of 6–8. According to the literature [59], MB is maximally adsorbed at pH ≥ 7, while BCG is maximally adsorbed at pH < 3. At lower pH, strong acidic conditions may cause partial dissolution or hydrolysis of functional groups on the hydrochar surface and can

lead to deformation of the adsorbent, while at higher pH, strong alkalinity can cause dye degradation.

The poor adsorption of MB at low pH indicates that π-π interactions play only a minor role in its adsorption. The adsorption of MB, a cationic dye, occurs via electrostatic and hydrogen-bond interactions [57], as the zeta potential decreases with increasing pH and the functional groups on the surface of the adsorbent become negatively charged due to deprotonation. This leads to improved electrostatic interactions and enhanced diffusion into the pores. The nitrogen of the MB dye and the OH groups of the adsorbent connect via hydrogen bonds [60]. When the adsorbent and adsorbate have opposite charges, electrostatic attraction occurs, which enhances dye adsorption. However, when they have the same charge (positive or negative), electrostatic repulsion occurs, reducing adsorption efficiency [61]. Other studies have also shown that increasing the pH promotes MB adsorption. For example, an alkaline pH was effective for MB adsorption by KOH-activated hydrochar from sewage sludge and coconut shells [26], as well as for MB adsorption by biochar composites from food waste digestate [62].

The pH of the solution also affects the ionization state of the MB or BCG molecules depending on their pKa value [61]. This influences the behaviour of the molecules, including their solubility and interaction with other substances, and explains the changes in removal efficiency mentioned above. The pKa value of MB, which is considered a cationic dye, is around 3.8 [60], so MB is in the protonated (charged) form at pH below 3.8, while it is in the deprotonated (neutral) form above this value. In contrast, BCG is an anionic dye with a pKa value of around 4.8 [9]; therefore, its adsorption is higher at lower pH, where protonation of surface functional groups creates positively charged sites that favour anion binding. An increase in pH results in a negatively charged adsorbent, which reduces adsorption efficiency due to electrostatic repulsion [19]. In addition to electrostatic effects, solubility, and π–π interactions between the dye's aromatic rings and the hydrochar matrix also contribute to the observed pH-dependent behaviour.

3.2.3 Parameters of the adsorption isotherms

The experimental isotherm data (equilibrium adsorption capacity versus equilibrium concentration) obtained during the adsorption of MB and BCG by unmodified and modified hydrochars are shown in Fig. 4. The adsorption isotherms for the Freundlich, Langmuir, Dubinin-Radushkevich, Toth, and Redlich-Peterson model equations are presented separately in the Supplementary material in Figures A.2 and A.3. The values of the calculated isotherm parameters and the corresponding R^2 values are summarised in Table 4.

Regarding the relevance of the kinetic models, the highest correlations for MB adsorption were observed for the Toth and Redlich-Peterson models, while for BCG adsorption the Redlich-Peterson and Freundlich models provided the best fit. The Redlich-Peterson, Freundlich, and Toth models reflect heterogeneous adsorption [43], involving multiple types of active sites with different affinities for dye molecules. This suggests that both physisorption and chemisorption processes contribute to overall uptake; therefore, dye adsorption occurs through multilayer and mixed-mechanism binding rather than uniform monolayer coverage. For all models, the correlation for BCG dye was higher than that for MB, indicating better predictability for this dye. The theoretical maximum adsorption capacities (q_m) calculated using the Langmuir, Toth, and Dubinin-Radushkevich models for specific samples were comparable to those determined experimentally for both MB and BCG adsorption. The correlation coefficients of the adsorption isotherms were highly dependent on the type of adsorbent. Apart from hydrochar H-AV-800, the correlation coefficients for all other adsorbents in the case of MB adsorption were above 0.9, indicating a high degree of agreement between the kinetic models and the experimental data. For BCG adsorption, KOH-modified hydrochar (sample H-KOH-800) and unmodified hydrochar H showed the highest correlation values.

According to the calculated isotherm parameters (Table 4), the Freundlich isotherm sorption coefficient (K_f) increases significantly from the unmodified to the modified hydrochars, with the highest value found for sample H-KOH-800, followed by sample H-AV-800. This indicates, that these two samples have a much higher affinity for MB adsorption than the other samples. A similar trend was observed for BCG. The Langmuir equilibrium adsorption constant (K_L) was highest for sample H-KOH-800, reflecting its strong binding affinity compared to the other adsorbents. The K_L values vary less for BCG than for MB adsorption. The Freundlich nonlinearity factor of heterogeneity (n) generally increases for modified samples, reflecting a diverse range of adsorption sites, while the Toth model parameter (n) remains relatively similar and much lower. The Redlich-Peterson model exponent n suggests near-Freundlich-like behaviour for certain adsorbents (e.g. H-800 and H-AV-800) and Langmuir-like behaviour for others (e.g. H-KOH-800).

The Dubinin-Radushkevich adsorption energy constant (K_D) varied considerably between samples, with no specific trend observed. The limited performance of the Dubinin-Radushkevich model is due to its primary restriction to describing adsorption in microporous materials, without accounting for surface heterogeneity or multi-layer adsorption. Additionally, it assumes a uniform Gaussian energy distribution of adsorption sites and disregards the complex

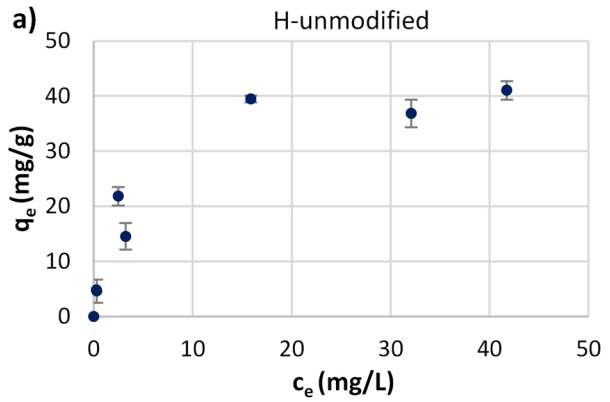
a)
H-unmodified
q_e (mg/g)
c_e (mg/L)

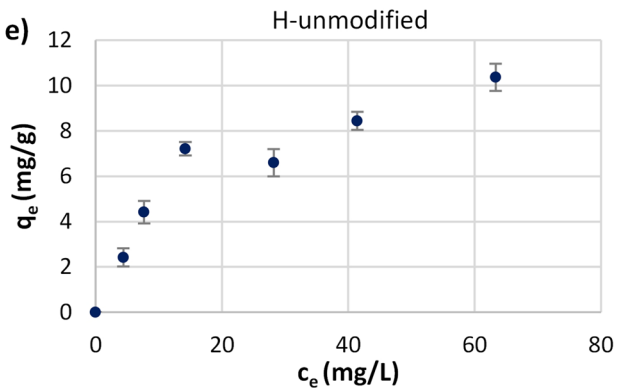
e)
H-unmodified
q_e (mg/g)
c_e (mg/L)

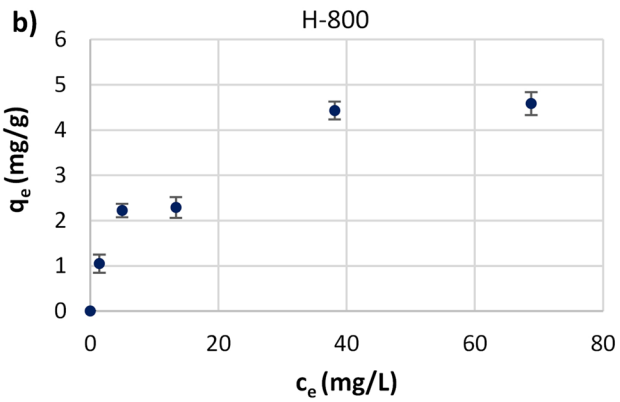
b)
H-800
q_e (mg/g)
c_e (mg/L)

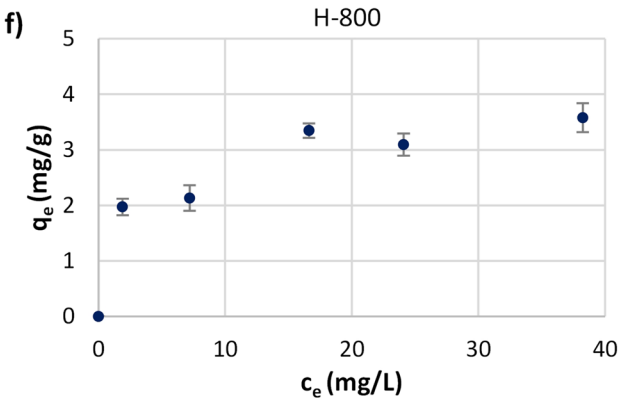
f)
H-800
q_e (mg/g)
c_e (mg/L)

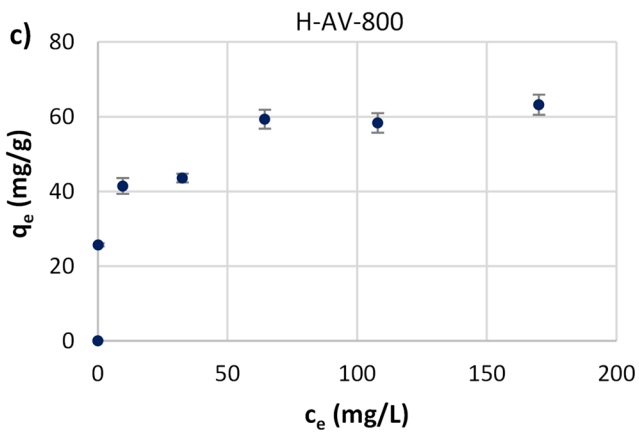
c)
H-AV-800
q_e (mg/g)
c_e (mg/L)

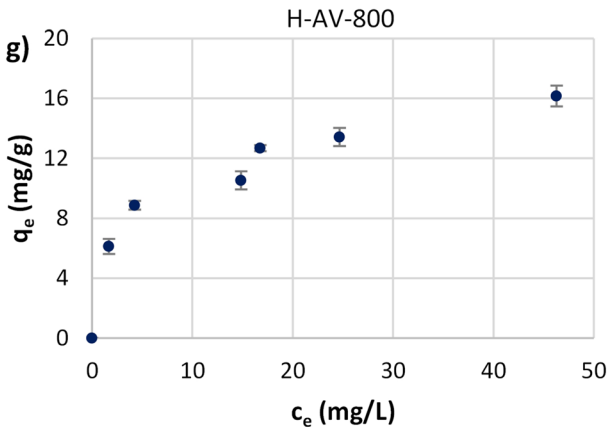
g)
H-AV-800
q_e (mg/g)
c_e (mg/L)

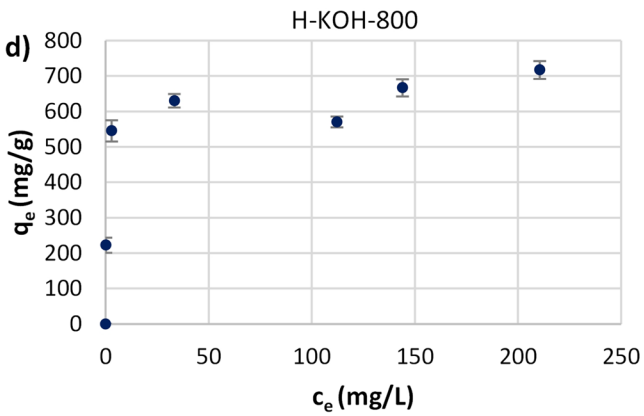
d)
H-KOH-800
q_e (mg/g)
c_e (mg/L)

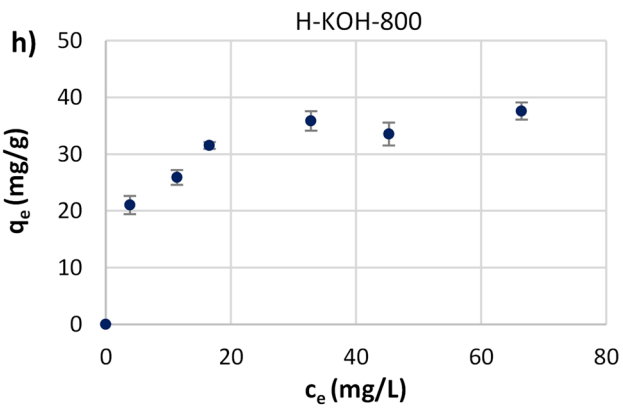
h)
H-KOH-800
q_e (mg/g)
c_e (mg/L)

Fig. 4 Experimental isotherm data (equilibrium adsorption capacity vs. equilibrium concentration) for unmodified (sample H) and modified hydrochars (samples H-800, H-AV-800 and H-KOH-800) exposed to adsorption of MB (**a**-**d**) and BCG (**e**-**h**)

energetics of real adsorption surfaces. For this reason, it performs poorly for adsorbents with different pore structures and considerable chemical interactions between adsorbate and adsorbent and is more suitable for physical adsorption than for chemisorption. The Redlich-Peterson, Toth, and Langmuir models are more flexible and can cover a wider range of adsorption systems, resulting in better correlations with experimental data. The Langmuir model assumes simple monolayer adsorption on a homogeneous surface with identical adsorption sites [63], whereas the Toth model describes non-ideal adsorption and is suitable for heterogeneous adsorption [43], as it includes a surface heterogeneity parameter that allows isotherms deviating from ideal behaviour to be described and is therefore effective for both low and high concentration ranges.

The Redlich-Peterson model, by contrast, combines features of the Langmuir and Freundlich models [64], with an empirical exponent that compensates for deviations from ideal conditions and fits exceptionally well, consistently yielding high R^2 values, as it can describe both monolayer and heterogeneous adsorption. However, H-KOH-800 is the most effective adsorbent overall, particularly for MB adsorption, due to its enhanced surface properties and the availability of functional groups, as it consistently exhibits the highest adsorption capacities and equilibrium constants. The maximum adsorption capacity of H-KOH-800 hydrochar determined using the Langmuir kinetic model, was 640.15 mg/g for MB adsorption and 38.17 mg/g for BCG adsorption. The markedly higher adsorption of MB compared to BCG is mainly due to differences in the molecular charge, size, and structure of the dyes. MB is smaller and cationic, allowing strong electrostatic attraction and π–π interactions with the negatively charged, aromatic surface of the modified hydrochars. In contrast, BCG is a larger, anionic molecule, which undergoes electrostatic repulsion and experiences steric hindrance within the pore network, resulting in a much lower adsorption capacity.

H-AV-800 hydrochar was the second most effective overall and the most effective among the acid-based modified hydrochars. Although it does not achieve the same adsorption efficiency as the KOH-modified hydrochar, its maximum adsorption capacities were still encouraging: 15.45 mg/g for BCG and 62.16 mg/g for MB adsorption. In comparison, the maximum adsorption capacity of unmodified hydrochar H was 12.61 mg/g for BCG and 44.30 mg/g for MB dye.

3.2.4 Comparison of adsorption capacities with recent studies

Comparison with the literature (Table 5) showed that the adsorption capacities achieved in this study are comparable to those reported in previous studies. Coconut husk and sewage sludge hydrochar activated with KOH and pyrolyzed achieved a maximum adsorption capacity for MB of 623 mg/g and for Congo red dye of 230 mg/g [26]. In contrast, pine wood sawdust biomass pre-treated with acids and subjected to a similar modification process (initial HTC treatment, followed by KOH activation and pyrolysis) showed half as high (303 mg/g) [65]. The adsorption of BCG was also less efficient than that of MB in other studies. Reported maximum adsorption capacities for BCG range from 33 mg/g for corncob biochar [19] or rice straw and husks-derived biochars [59], up to 99 mg/g for biochar from cucumber straw [61]. None of the studies on BCG adsorption used hydrochar or modified hydrochar as the adsorbent. Among natural modifiers, only one study on activation with coconut vinegar was found, but this related to the adsorption of Ca^{2+} ions rather than dyes. Modification with other organic acids, referred to as 'natural organic acids', has also been shown to be effective; for example, modification of biochar with citric acid resulted in a maximum adsorption capacity for MB dye of 395 mg/g [66]. There is also a study on the application of sunflower oil cake pre-treated with H_2SO_4 and pyrolyzed at 600 °C for MB adsorption, with a maximum adsorption capacity of 16.4 mg/g [31], but no study on the use of hemp cake hydrochar for this purpose.

3.2.5 Adsorption mechanism and surface properties of adsorbents

The predominant adsorption mechanism for a specific pollutant depends on the properties of the adsorbent, with the main factors being surface area, porosity, and the functional groups present on the adsorbent surface, as well as the properties and functional groups of the adsorbate (i.e. the dye), and the adsorption conditions (pH, temperature, etc.) [60]. Dye adsorption most commonly occurs via mechanisms such as hydrogen bonding, π–π interaction [71], electrostatic attraction, and pore filling [27]. The FTIR spectra (Fig. 5) recorded before and after adsorption of MB and BCG confirmed the successful adsorption of dyes on the tested adsorbents.

The FTIR profiles of the modified adsorbents exhibited changes similar to those of the unmodified adsorbent after dye adsorption. These changes include peak shifts, variations in intensity, and even the disappearance of peaks, indicating various chemical changes on the adsorbents due to

Table 4 The isotherm parameters of the Langmuir, Freundlich, Dubinin-Radushkevich, Toth, and Redlich-Peterson model equations for the adsorption of MB and BCG on modified hydrochars

Model	Parameter	Methylene blue (MB)				Bromocresol green (BCG)			
		H	H-800	H-AV-800	H-KOH-800	H	H-800	H-AV-800	H-KOH-800
Freundlich	K_F [(mg/g)(mg/L)^n]	0.7431	1.0811	27.6562	394.0607	1.4116	1.5982	5.4859	17.0101
	n	0.3922	2.8249	6.1575	9.2908	2.0896	4.5098	3.5786	5.1861
	R^2	0.9241	0.9620	0.7636	0.9290	0.9891	0.9672	0.9875	0.9819
Langmuir	K_L (L/mg)	0.2642	0.1075	0.1616	3.7507	0.0531	0.4671	0.3003	0.2703
	q_m (mg/g)	44.30	5.16	62.16	640.15	12.61	3.52	15.45	38.17
	R^2	0.9566	0.9419	0.7465	0.9684	0.9733	0.9355	0.9516	0.9818
Dubinin-Radushkevich	K_D (mol^2/kJ^2)	0.0951	0.1504	0.1664	0.018	0.2694	0.0579	0.0790	0.1003
	q_m (mg/g)	42.72	4.51	60.91	647.91	10.34	3.42	14.68	37.20
	R^2	0.9482	0.8981	0.7422	0.9733	0.9543	0.9292	0.9403	0.9773
Toth	K_T (L/mg)	0.2314	0.1864	0.3439	8.698	0.0620	1.8545	0.2919	0.8141
	q_m (mg/g)	42.61	8.56	64.66	666.59	18.60	4.42	20.62	44.46
	n	1.1934	0.4591	0.6955	0.6082	0.5846	0.478	0.6393	0.5034
	R^2	0.9568	0.9602	0.7522	0.9752	0.9826	0.9564	0.9604	0.9493
Redlich-Peterson	K_{RP} (L/g)	13.44	2.60	74.93	993.45	16.69	3.08	24.19	18.99
	a (L/mg)	0.3706	1.8423	2.5001	1.5304	11.239	1.3958	3.8276	0.7579
	n	0.9467	0.7057	0.8531	0.9981	0.5315	0.8599	0.7563	0.8978
	R^2	0.9549	0.9638	0.7629	0.9419	0.9891	0.9575	0.9876	0.9862

interactions between the adsorbent and the adsorbate. Significant changes were observed, particularly for OH, NH, and CH groups, C = O groups, and groups representing aromatic rings. The peaks at about 3400 cm^{-1} and 1600 cm^{-1}, which indicate hydrogen-bonding interactions between –OH and –C = O groups in the COOH of the hydrochar and the dye, shifted. More precisely, hydrogen bonding occurs between the nitrogen originating from the dye and the oxygen from the carboxyl (–OH) or carbonyl (–C = O) groups of the adsorbent, and between the nitrogen and the hydrogen from the carboxyl (–OH) or amine ($–NH_2$) group [33]. In the case of MB adsorption, particularly in samples H-KOH-800 and H-AV-800, a new peak appears at around 1500 cm^{-1} or its intensity increases, indicating the presence of C = C and C = N bonds, so-called π–π interactions between the aromatic ring (–C = C–) of the hydrochar, acting as π-electron donor, and the aromatic groups of the dye, acting as π-electron acceptors [59]. The π–π interactions are strongly influenced by the polarity and aromaticity of the adsorbents, which are directly related to the O/C and H/C ratios. In addition to H-bonding and π–π interactions, electrostatic interactions also occur. The electrostatic attraction between the negatively charged surface (O^- of carbonyl, carboxyl or amine groups) of the adsorbent and the positively charged cations in the MB dye (N^+ in the dye) may be one of the driving forces in adsorption [60], as the electrostatic attraction between the hydrochar surface and the MB dye molecules increases with increasing pH, resulting in higher adsorption efficiency. For the BCG dye, which is an anionic dye, the opposite effect occurs, as electrostatic interactions are promoted under acidic conditions in the solution [61]. The adsorption of BCG on samples H-AV-800 and H-KOH-800 is indicated by the shift of the peak at approximately 1600 cm^{-1} (C = O group) to lower wavenumbers, and the peak also becomes broader. In contrast, very little change is observed in the FTIR spectra of sample H-800, indicating poor adsorption performance. For the hydrochars modified with KOH and alcoholic vinegar, the mechanism of pore filling, which is controlled by the pore volume, could also play an important role in the removal of dyes from water solutions, as these two adsorbents have the highest pore volume and quite large pores according to BET (see Table 2) and SEM-EDS analysis (Fig. 6).

The SEM images of the unmodified hydrochar H and the modified hydrochars H-AV-800 and H-KOH-800 showed several differences in the morphology and structure of the materials resulting from the modification. Sample H-KOH-800 had the most porous structure of all samples, with clearly recognisable pores ranging from 30 to 1160 nm, while sample H-AV-800 was more compact and had pores ranging from 200 to 900 nm, with various particles observed on the surface of the material. On the other hand, unmodified hydrochar consisted of the smallest particles, with the white areas most likely representing fat residues in the sample. This indicates that KOH activation produces a highly porous, open structure, while vinegar treatment results in moderate porosity with smoother surfaces. These morphological differences correspond to the adsorption capacities: H-KOH-800 > H-AV-800 > H-WV-800 > H > H-800 > H-AA-800. The improved pore structure facilitates enhanced diffusion and surface interactions. Otherwise, the morphological properties of the tested hydrochars were consistent with those of modified pyrochars and hydrochars

Table 5 Comparison of the adsorption capacities of adsorbents derived from hemp oil cake in this study with the adsorption capacities for MB, BCG, and other pollutants in studies on the adsorption and modification of adsorbents

Type of biomass	Method of production of adsorbent	Method/type of chemical modification of biochar	Amount of adsorbent and contact time	Adsorbate and adsorption capacity	Reference
Hemp oil cake	HTC (250 °C, 5 h)	Activation by: a) alcoholic vinegar (16 h), b) 60% KOH (16 h). After activation, the samples were exposed to pyrolysis at 800 °C (1 h).	0.01–0.1 g/50 mL of dye solution (96 h)	MB: 44.30 mg/g (unmodified hydrochar), 62.16 mg/g (vinegar-modified), 640.15 mg/g (KOH-modified) BCG: 12.61 mg/g (unmodified hydrochar), 15.45 mg/g (vinegar-modified), 38.17 mg/g (KOH-modified)	This study
Eucalyptus saw dust	First, the biomass was pre-treated with a specific acid (citric, tartaric, or acetic) at the chosen impregnation ratios. The material was then dried at 50 °C for 24 h and subsequently exposed to low-temperature modification at 120 °C for 90 min.	/	0.1 g/200 mL (2 h)	MB 178.57 mg/g (citric acid-modified), 99.01 mg/g (tartaric acid-modified), 29.94 mg/g (acetic acid-modified)	[48]
Lingocellulosic biomass (remains of olives after pruning, coffee husks)	Pyrolysis (500 °C, 2 h)	K_2CO_3 (2 g/g) or KOH (80%)	1 g/L (5 h)	MB (312–1000 mg/g)	[50]
Coconut husk, sewage sludge	HTC (140–240 °C, 1–7 h)	KOH activation (1–4 mol/L), followed by pyrolysis (900 °C, 70 min)	0.6 g/L (12 h)	MB (623 mg/g), Congo red (230 mg/g)	[26]
Pine wood sawdust	Pre-treatment of biomass with acids (citric, tartaric, formic acid, H_3PO_4, all at 10%), followed by HTC treatment (210 °C, 24 h)	KOH activation (6 g/40 mL H_2O, 6 h), followed by pyrolysis at 1000 °C (2 h)	0.02 g/20 mL (6 h)	MB (303 mg/g)	[65]
Sunflower oil cake	Pre-treatment with H_2SO_4, followed by pyrolysis 600 °C (1 h)	/	0.02 g/10 mL (24 h)	MB (16.4 mg/g)	[31]
Water hyacinth	Pyrolysis (300 °C, 2 h)	Modification with 0.6 M citric acid (2 h), followed by drying at 120 °C	50 mg/50 mL (24 h)	MB (395 mg/g)	[66]
Food waste digestate	Pyrolysis (500–1000 °C, 3 h)	/	0.2 g/50 mL (49 h)	MB (up to 1123.5 mg/g)	[62]
Hemp seed nanoparticle composites	A one-pot synthesis method was used to prepare composites composed of hemp seed and either $Mn(NO_3)_2{\cdot}4H_2O$ or $Cu(NO_3)_2{\cdot}5H_2O$. The mixture was heated at 45 °C for 2 h, followed by a 12-hour reaction and drying (24 h)	/	20 mg/50 mL (5–1440 min)	MB (up to 68.95 mg/g)	[33]
Fruit peels	HTC method (200 °C, 10 h)	/	10 mg/50 mL (30 min)	MB (up to 21 mg/g)	[63]
Rice straw, rice husk	Pyrolysis (300–700 °C, 2 h)	Modification with 0.1 M HCl (1 h), washing and drying at 80 °C overnight	0.01–0.05 g/10 mL (12 h)	BCG and MB (32,81 − 67,69 mg/g)	[59]
Corn cob	Corn cob was pre-treated with 45% H_3PO_4 at an acid/biomass ratio of 4:1 at 120 °C for 24 h. The sample was then pyrolyzed at 700 °C for 5 h.	/	0.1–2 g/200 mL (10–60 min)	BCG (34.41–41.94 mg/g)	[19]
Cucumber Straw	Pyrolysis (600 °C, 2 h)	/	0.02–0.1 g/50 mL (60 min)	BCG (99.18 mg/g)	[61]

Table 5 (continued)

Type of biomass	Method of production of adsorbent	Method/type of chemical modification of biochar	Amount of adsorbent and contact time	Adsorbate and adsorption capacity	Reference
Corn straw, corn cobs	a) Pyrolysis (350–500 °C, 2 h) b) HTC (200 °C, 5 h) c) HTC (200 °C, 5 h), followed by pyrolysis (350–500 °C, 2 h)	/	0.3 g/50 mL (50–200 h)	Atrazine (3.2 mg/g), Cd^{2+} (15.6 mg/g), Cr(VI) (4.2 mg/g)	[67]
Wood (hickory), peanut husks	HTC (200 °C, 6 h)	a) KOH activation (50% KOH, ratio biochar/KOH 1:1), heating (85 °C, 2 h), drying (100 °C, 24 h), then pyrolysis (600 °C, 1 h), b) Activation with H_3PO_4 (85%) according to the same procedure as KOH activation	10 mg (1 h)	Acetone, Cyclohexane (51–160 mg/g)	[68]
Sewage sludge digestate	Pyrolysis, 800 °C (2 h)	Activation with citric acid (0.3 M, 2 h), then evaporation (50 °C, 4 h) and drying (100 °C, 4 h)	0.4 g/L (24 h)	Tetracycline (58.25 mg/g)	[38]
Palm kernel husks	First HTC treatment (200 °C, 4 h), followed by activation by pyrolysis (400 °C, 4 h)	/	1.5 g/100 mL (1.5 h)	Diclofenac (13.16 mg/g)	[69]
Wood biomass	Pyrolysis (300 °C, 2 h)	Activation with coconut vinegar (biochar/vinegar 1:2 v/v, soaking for 24 h, then drying at 120 °C (5 h), rinsing with distilled water and drying at 80 °C (12 h)	0.1 g/20 mL (1 h)	Ca^{2+} (9.9 mg/g)	[37]
Acidic vinegar residue	Pyrolysis (700 °C, 2 h)	Modification with $ZnCl_2$	20 mg/10 mL (24 h)	Cr (VI) (236.8 mg/g)	[70]

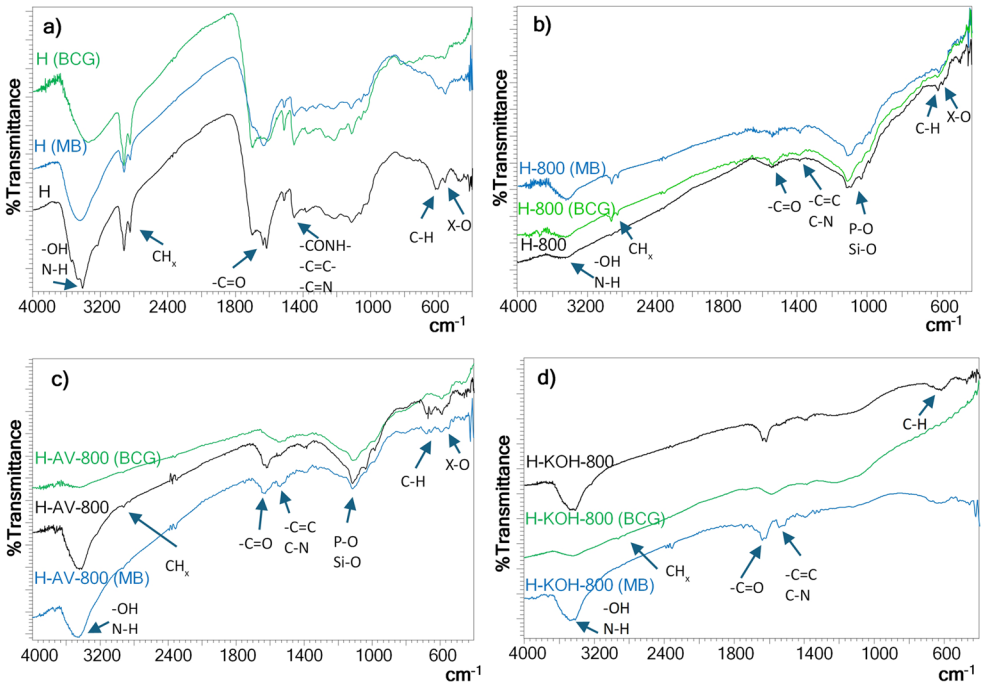

Fig. 5 FTIR spectra, recorded before and after adsorption of MB and BCG, for hydrochars: (**a**) H, (**b**) H-800, (**c**) H-AV-800, and (**d**) H-KOH-800

obtained from materials such as corn straw or corn cobs [67]. The results of the SEM-EDS analysis, summarised in Table 6, show that, in addition to the basic elements identified by elemental analysis, various other elements are present on the surface of the adsorbents, which may also participate in the adsorption of MB and BCG. According to the EDS analysis, the samples contained a high proportion of carbon (sample H-KOH-800: 69–80 wt%, sample H-AV-800: 74–86 wt%,

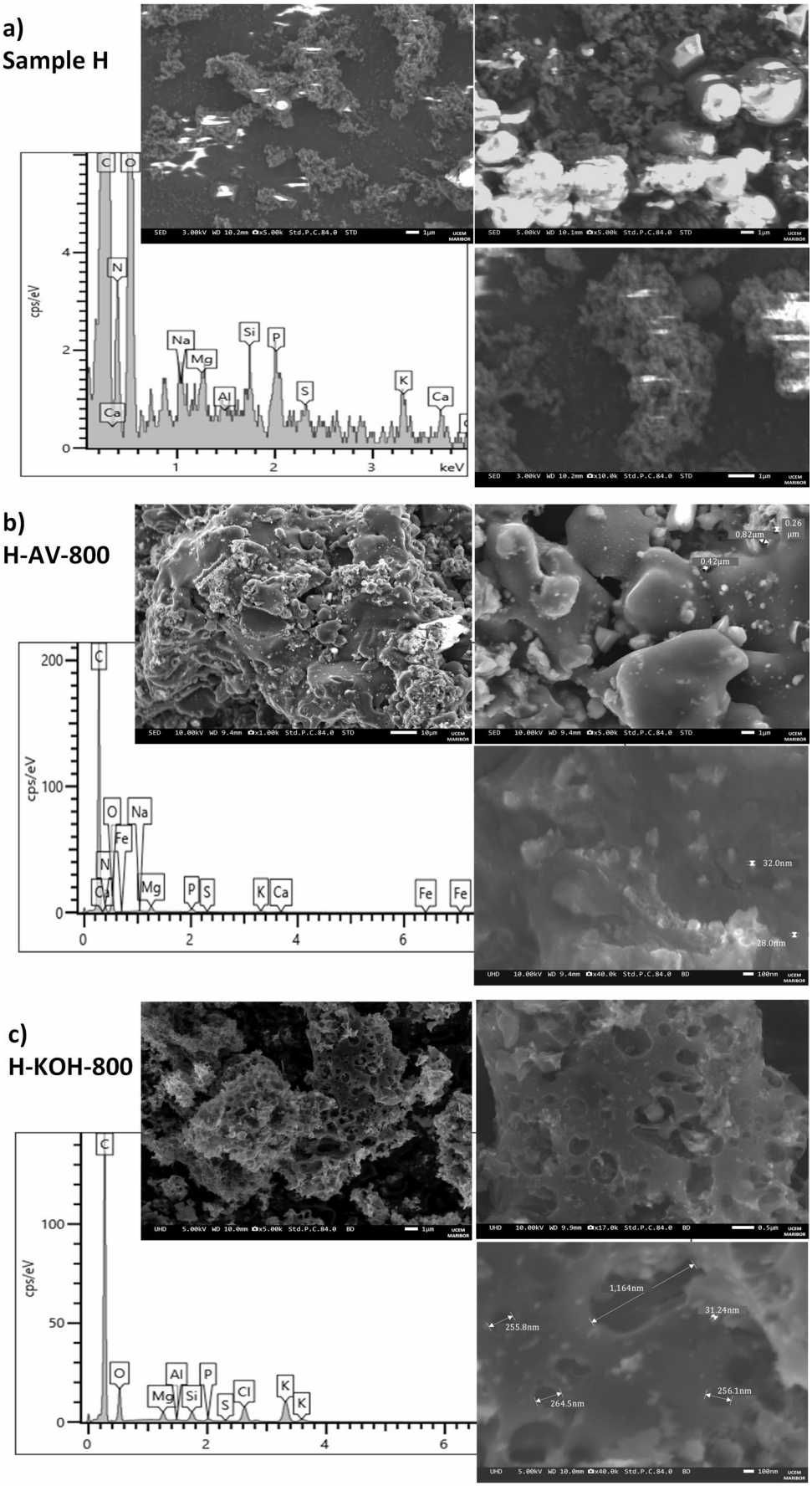

Fig. 6 SEM images and SEM-EDS spectra of unmodified hydrochar H (**a**), and thermo-chemically modified hydrochars H-AV-800 (**b**) and H-KOH-800 (**c**)

Table 6 Results of the SEM-EDS analysis of samples H, H-AV-800 and H-KOH-800

Sample	Spectrum	Element													
		C (wt%)	N (wt%)	O (wt%)	Na (wt%)	Mg (wt%)	Al (wt%)	Si (wt%)	P (wt%)	S (wt%)	K (wt%)	Ca (wt%)	Fe (wt%)	Cl (wt%)	Total (wt%)
H	Spectrum 1	83.63	1.57	10.81	0.35	0.27	0.08	0.38	0.77	0.31	0.99	0.85	/	/	100
	Spectrum 2	83.26	3.06	10.60	/	0.37	/	0.20	0.95	0.15	0.67	0.74	/	/	100
	Spectrum 3	78.63	7.51	12.17	0.12	0.17	/	0.09	0.56	0.21	0.55	/	/	/	100
	Spectrum 4	80.70	7.56	11.42	/	/	/	/	/	0.31	/	/	/	/	100
H-AV-800	Spectrum 1	86.28	3.75	5.96	0.10	1.01	/	/	0.80	0.25	1.42	0.43	/	/	100
	Spectrum 2	79.59	5.68	8.77	0.20	1.17	/	/	1.29	0.26	1.55	1.49	/	/	100
	Spectrum 3	73.68	10.88	10.98	0.13	1.22	/	/	1.10	0.14	1.11	0.48	0.27	/	100
	Spectrum 4	79.67	7.80	9.21	0.15	0.83	/	/	0.80	0.16	1.07	0.31	/	/	100
H-KOH-800	Spectrum 1	75.00	0.90	11.27	/	0.82	/	1.46	0.58	/	8.15	/	/	1.81	100
	Spectrum 2	80.13	0.67	6.64	/	0.29	/	0.34	0.28	/	9.43	/	/	2.21	100
	Spectrum 3	73.78	0.58	14.38	/	0.92	0.12	2.10	0.64	/	6.14	/	/	1.34	100
	Spectrum 4	66.79	/	10.15	/	2.02	0.24	5.87	1.65	/	10.21	0.96	/	2.11	100
	Spectrum 5	69.10	/	12.23	/	1.10	0.06	1.43	0.45	0.08	10.88	/	/	4.68	100
	Spectrum 6	71.23	/	14.52	/	1.27	0.08	1.7	0.55	0.07	8.21	/	/	2.38	100

and sample H: 79–84 wt%), as well as oxygen and nitrogen, consistent with the elemental analysis. Elements such as P, S, Si, Na, Mg, Al, Ca, and Fe were present in trace amounts and not in all samples. Al was observed in samples H and H-KOH-800, while Fe was detected only in sample H-AV-800. As expected, the H-KOH-800 sample contained a much higher K content, and Cl was also detected in this sample, as the hydrochar was washed with dilute HCl after KOH modification. The results of the FTIR, SEM-EDS, and BET measurements, as well as the kinetic parameters obtained from the kinetic analysis, indicate that different adsorption mechanisms acting synergistically are involved in the adsorption of MB and BCG dye. Similar findings have been reported in previous studies on the adsorption of dyes, including cationic dyes such as MB and anionic dyes such as acid orange [27].

3.2.6 Challenges in dye adsorption, regeneration of adsorbents and environmental acceptability

The challenges in adsorption-based wastewater treatment and scaling up dye removal using modified biochars in real systems encompass multiple interlinked issues [72]. These include improving the effectiveness, capacity, and selectivity of adsorbents; potential leaching and toxicity of residual modifiers (e.g. KOH, organic acids) into treated water; sustainability limitations; loss of performance or structural degradation during repeated regeneration cycles; competition from natural organic matter and competing ions in complex wastewater matrices; mass transfer limitations and hydrodynamic constraints; variability in biomass feedstocks and chemical modifiers affecting reproducibility in the production of biomass-derived adsorbents; and the trade-off between regeneration efficacy and secondary waste generation. Addressing these challenges requires rigorous post-treatment washing validation and ecotoxicity assays, pilot-scale column studies with breakthrough modelling, and techno-economic and life cycle assessments (LCA) to ensure sustainable scalability. An in-depth review of the most recent literature and findings on LCA and techno-economic evaluation of the use of modified hydrochar for pollution remediation, including dyes and heavy metals, was conducted by Saba et al. [73]. According to their findings, techno-economic analyses of the production of modified adsorbents from valorized wastes demonstrate techno-economic benefits and can be recognised as sustainable applications compared to other commercial adsorbents.

Regarding the toxicity of modified hydrochars, neither the natural modifiers (such as vinegar) nor their potential degradation products are considered toxic at the residual concentrations expected in the adsorbents, particularly after high-temperature modification. Furthermore, no heavy metals or other harmful elements were detected in the adsorbent

modified with vinegar, according to SEM-EDS analysis. Therefore, when using natural modifiers, no significant leaching or toxicity is expected, and the materials can be regarded as environmentally safe for water treatment applications. This conclusion aligns with recent findings for similarly prepared green-modified hydrochars [51]. In contrast, the KOH-modified adsorbent contained a considerable amount of potassium and chlorides, but no toxic heavy metals. However, leaching in the case of the KOH modifier can be prevented by additional washing of the adsorbent with dilute acid and distilled water.

According to previous studies, the regeneration of such adsorbents is possible using various methods, including conventional desorption techniques such as chemical desorption with acids, bases, alcohols, and other reagents, as well as thermal desorption [74]. Recently, various novel methods have been tested, including microwave, ultrasonic, supercritical water or carbon dioxide regeneration, and electrochemical regeneration [75]. These methods can efficiently recover the adsorbents, although their adsorption performance usually decreases after several regeneration cycles. Although regeneration was not included in this study, it should be investigated in the future before the potential use of modified adsorbents.

4 Conclusions

In this study, the efficiency of unmodified and thermo-chemically modified hydrochars from hemp oil cake and whey in adsorbing MB and BCG dyes was investigated. Chemical and surface analyses revealed several changes in the chemical and surface properties of the hydrochars resulting from thermo-chemical modification. Modification with natural vinegars was more effective than modification with acetic acid, but less effective than modification with KOH in improving surface area and porosity. However, it introduced additional acidic functional groups on the surface of the hydrochars, which contributed to enhanced adsorption through improved interactions between the adsorbent and dyes. Among the acid-treated samples, hydrochar modified with alcoholic vinegar exhibited the highest adsorption efficiency and the greatest capacity for MB and BCG dyes. Conventional alkali (KOH)-treated hydrochar showed the highest adsorption capacity among all samples, due to a significant increase in surface area and porosity. Adsorption efficiency was strongly influenced by pH, with MB adsorption promoted under alkaline conditions and BCG adsorption under acidic conditions. The isotherm kinetic models indicated heterogeneous adsorption, with the Redlich-Peterson and Freundlich models being the most suitable. The main adsorption mechanisms included electrostatic interactions, hydrogen bonding, π–π interactions and pore filling. The results highlight the potential of thermo-chemically modified hydrochars from hemp oil cake as sustainable adsorbents for dye removal from aqueous solutions and show that natural modifiers can improve the adsorption performance of hydrochars, although they are less efficient than conventional modifiers.

Supplementary Information The online version contains supplementary material available at https://doi.org/10.1007/s13399-025-07017-2.

Acknowledgements The authors thank the Slovenian Research Agency (ARIS) for financially supporting this study. Part of the experimental work was carried out using instruments provided by the project "Upgrading national research infrastructures - RIUM", co-financed by the Republic of Slovenia, the Ministry of Education, Science and Sport, and the European Union from the European Regional Development Fund.

Author contributions Aleksandra Petrovič: writing – original draft, conceptualization, investigation, methodology, visualization. Patricija Završki: writing – original draft, formal analysis, visualization. Muzafera Paljevac: formal analysis, investigation, validation. Sabina Vohl: methodology, data curation, formal analysis. Lidija Čuček: funding acquisition, writing – review and editing, supervision. Marjana Simonič: resources, writing – review and editing, supervision.

Funding This research was financially supported by the Slovenian Research Agency (ARIS): funding of research programmes No. P2-0006, P2-0414, P2-0421 and project J4-50149.

Data availability The original contributions presented in the study are included in the article; additional queries regarding the data can be addressed to the corresponding author.

Declarations

Conflict of interest The authors have no competing interests to declare that are relevant to the content of this article.

References

1. Al-Tohamy R, Ali SS, Li F, Okasha KM, Mahmoud YAG, Elsamahy T, Jiao H, Fu Y, Sun J (2022) A critical review on the treatment of dye-containing wastewater: ecotoxicological and health concerns of textile dyes and possible remediation approaches for

environmental safety. Ecotoxicol Environ Saf 231:113160. https://doi.org/10.1016/j.ecoenv.2021.113160
2. Pandit P, Singha K, Maity S, Maiti S, Kane P (2021) Chapter Six - Treatment of textile wastewater by agricultural waste biomasses. In: Muthu SS (ed) Sustainable Technologies for Textile Wastewater Treatments. Woodhead Publishing, pp 137–156
3. Mihai S, Bondarev A, Necula M (2025) The potential of biogenic materials as sustainable and environmentally benign alternatives to conventional adsorbents for dyes removal: a review. Processes. https://doi.org/10.3390/pr13020589
4. Modi S, Yadav VK, Gacem A, Ali IH, Dave D, Khan SH, Yadav KK, Rather S-u, Ahn Y, Son CT, Jeon B-H (2022) Recent and emerging trends in remediation of methylene blue dye from wastewater by using zinc oxide nanoparticles. Water 14(11):1749. https://doi.org/10.3390/w14111749
5. Lellis B, Fávaro-Polonio CZ, Pamphile JA, Polonio JC (2019) Effects of textile dyes on health and the environment and bioremediation potential of living organisms. Biotechnol Res Innov 3(2):275–290. https://doi.org/10.1016/j.biori.2019.09.001
6. Singha K, Pandit P, Maity S, Sharma SR (2021) Chap. 11 - Harmful environmental effects for textile chemical dyeing practice. In: Ibrahim N, Hussain CM (eds) Green Chemistry for Sustainable Textiles. Woodhead Publishing, pp 153–164
7. Maheshwari K, Agrawal M, Gupta AB (2021) Dye Pollution in Water and Wastewater. In: Muthu SS, Khadir A (eds) Novel Materials for Dye-containing Wastewater Treatment. Springer Singapore, Singapore, pp 1–25
8. Bal G, Thakur A (2022) Distinct approaches of removal of dyes from wastewater: a review. Mater Today Proc 50:1575–1579. https://doi.org/10.1016/j.matpr.2021.09.119
9. Revilla Pacheco C, Riveros Cruz MR, Cárdenas Garcia J, Terán Hilares R, Colina Andrade GdJ, Pacheco Tanaka DA, Mogrovejo-Valdivia A (2023) Adsorption and degradation of rhodamine B and bromocresol green by FeOCl under advanced oxidation process. Arab J Chem 16(9):105049. https://doi.org/10.1016/j.arabjc.2023.105049
10. Mohammadzadeh Pakdel P, Peighambardoust SJ (2018) Review on recent progress in chitosan-based hydrogels for wastewater treatment application. Carbohydr Polym 201:264–279. https://doi.org/10.1016/j.carbpol.2018.08.070
11. Foroughi M, Peighambardoust SJ, Ramavandi B, Boffito DC (2024) Simultaneous anionic dyes degradation via H_2O_2 activation using Zeolite 4A/ZnO/$Fe_2(MoO_4)_3$ nanoparticles in a sono-photocatalytic process. Adv Powder Technol 35(1):104320. https://doi.org/10.1016/j.apt.2023.104320
12. Foroutan R, Peighambardoust SJ, Ghojavand S, Foroughi M, Ahmadi A, Bahador F, Ramavandi B (2024) Development of a magnetic orange seed/Fe3O4 composite for the removal of methylene blue and crystal violet from aqueous media. Biomass Convers Biorefin 14(20):25685–25700. https://doi.org/10.1007/s13399-023-04692-x
13. Zhou Y, Lu J, Zhou Y, Liu Y (2019) Recent advances for dyes removal using novel adsorbents: a review. Environ Pollut 252:352–365. https://doi.org/10.1016/j.envpol.2019.05.072
14. Saad H, El-Dien FAN, El-Gamel NEA, Abo Dena AS (2022) Azo-functionalized superparamagnetic Fe3O4 nanoparticles: an efficient adsorbent for the removal of bromocresol green from contaminated water. RSC Adv 12(39):25487–25499. https://doi.org/10.1039/D2RA03476J
15. Salmalian E, Rezaei H, Shahbazi A (2019) Removal of bromocresol green from aqueous solutions using chitin nanofibers. Environ Resour Res 7(2):79–86. https://doi.org/10.22069/ijerr.2019.4816
16. Dhanya V, Balaji D, Swetha A, Shri Vigneshwar S (2022) A comprehensive review of effective adsorbents used for the removal of dyes from wastewater. Curr Anal Chem 18(3):255–268. https://doi.org/10.2174/1573411016999200831111155
17. Huang W-H, Lee D-J, Huang C (2021) Modification on biochars for applications: a research update. Bioresour Technol 319:124100. https://doi.org/10.1016/j.biortech.2020.124100
18. Lan D, Zhu H, Zhang J, Li S, Chen Q, Wang C, Wu T, Xu M (2022) Adsorptive removal of organic dyes via porous materials for wastewater treatment in recent decades: a review on species, mechanisms and perspectives. Chemosphere 293:133464. https://doi.org/10.1016/j.chemosphere.2021.133464
19. Onu CE, Ohale PE, Ekwueme BN, Obiora-Okafo IA, Okey-Onyesolu CF, Onu CP, Ezema CA, Onu OO (2022) Modeling, optimization, and adsorptive studies of bromocresol green dye removal using acid functionalized corn cob. Cleaner Chemical Engineering 4:100067. https://doi.org/10.1016/j.clce.2022.100067
20. John KI, Omorogie MO (2022) Biomass-based hydrothermal carbons for catalysis and environmental cleanup: a review. Green Chem Lett Rev 15(1):162–186. https://doi.org/10.1080/17518253.2022.2028017
21. Nusrat T, Sharf Ilahi S, Geetanjali R, Saif Ali C, Inamuddin, Abdullah MA (2020) Nano-engineered adsorbent for the removal of dyes from water: A review. Curr Anal Chem 16(1):14–40. https://doi.org/10.2174/1573411015666190117124344
22. Uddin MJ, Ampiaw RE, Lee W (2021) Adsorptive removal of dyes from wastewater using a metal-organic framework: a review. Chemosphere 284:131314. https://doi.org/10.1016/j.chemosphere.2021.131314
23. Vishnu D, Dhandapani B, Kannappan Panchamoorthy G, Vo D-VN, Ramakrishnan SR (2021) Comparison of surface-engineered superparamagnetic nanosorbents with low-cost adsorbents of cellulose, zeolites and biochar for the removal of organic and inorganic pollutants: a review. Environ Chem Lett 19(4):3181–3208. https://doi.org/10.1007/s10311-021-01201-2
24. Akbari A, Peighambardoust SJ, Kazemian H (2025) Comparative study on the impact of physicochemical characteristics of the activated carbons derived from biochar/hydrochar on the adsorption performances. Environ Res 270:121022. https://doi.org/10.1016/j.envres.2025.121022
25. Emmanuel SS, Adesibikan AA (2024) Hydrothermal valorization of biomass waste into hydrochar towards circular economy and sustainable adsorptive dye contaminants clean-up: a review. Desalin Water Treat 320:100801. https://doi.org/10.1016/j.dwt.2024.100801
26. Tu W, Liu Y, Xie Z, Chen M, Ma L, Du G, Zhu M (2021) A novel activation-hydrochar via hydrothermal carbonization and KOH activation of sewage sludge and coconut shell for biomass wastes: preparation, characterization and adsorption properties. J Colloid Interface Sci 593:390–407. https://doi.org/10.1016/j.jcis.2021.02.133
27. Rawat S, Ahammed MM (2024) Clay-moringa seedcake composite for removal of cationic and anionic dyes. Chemosphere 350:141083. https://doi.org/10.1016/j.chemosphere.2023.141083
28. Merikhy A, Heydari A, Eskandari H, Ghahraman-Rozegar F (2020) Carbonized spent bleaching earth as a low-cost adsorbent: a facile revalorization strategy via response surface methodology. Chem Eng Process Process Intensif 158:108167. https://doi.org/10.1016/j.cep.2020.108167
29. Aragaw TA, Bogale FM (2021) Biomass-based adsorbents for removal of dyes from wastewater: a review. Front Environ Sci. https://doi.org/10.3389/fenvs.2021.764958
30. Jose S, Roy R, Phukan AR, Shakyawar DB, Anuradha S (2022) Biochar from oil cakes: an efficient and economical adsorbent for the removal of acid dyes from wool dye house effluent. Clean Technol Environ Policy 24(5):1599–1608. https://doi.org/10.1007/s10098-021-02253-2
31. Karagöz S, Tay T, Ucar S, Erdem M (2008) Activated carbons from waste biomass by sulfuric acid activation and their use on

methylene blue adsorption. Bioresour Technol 99(14):6214–6222. https://doi.org/10.1016/j.biortech.2007.12.019
32. Alshareef SA, Otero M, Alanazi HS, Siddiqui MR, Khan MA, Alothman ZA (2021) Upcycling olive oil cake through wet torrefaction to produce hydrochar for water decontamination. Chem Eng Res Des 170:13–22. https://doi.org/10.1016/j.cherd.2021.03.031
33. Mphuthi BR, Thabede PM, Monapathi ME, Shooto ND (2023) Hemp seed nanoparticle composites for removing lead, methylene blue, and ibuprofen from an aqueous solution and their antimicrobial towards *Escherichia coli* and *Staphylococcus aureus*. Case Studies in Chemical and Environmental Engineering 8:100436. https://doi.org/10.1016/j.cscee.2023.100436
34. Rajapaksha AU, Chen SS, Tsang DCW, Zhang M, Vithanage M, Mandal S, Gao B, Bolan NS, Ok YS (2016) Engineered/designer biochar for contaminant removal/immobilization from soil and water: potential and implication of biochar modification. Chemosphere 148:276–291. https://doi.org/10.1016/j.chemosphere.2016.01.043
35. Díaz B, Sommer-Márquez A, Ordoñez PE, Bastardo-González E, Ricaurte M, Navas-Cárdenas C (2024) Synthesis methods, properties, and modifications of biochar-based materials for wastewater treatment: a review. Resources 13(1):8. https://doi.org/10.3390/resources13010008
36. Peiris C, Nayanathara O, Navarathna CM, Jayawardhana Y, Nawalage S, Burk G, Karunanayake AG, Madduri SB, Vithanage M, Kaumal MN, Mlsna TE, Hassan EB, Abeysundara S, Ferez F, Gunatilake SR (2019) The influence of three acid modifications on the physicochemical characteristics of tea-waste biochar pyrolyzed at different temperatures: a comparative study. RSC Adv 9(31):17612–17622. https://doi.org/10.1039/C9RA02729G
37. Udawatta MM, De Silva RCL, De Silva DSM (2023) Surface modification of *Trema orientalis* wood biochar using natural coconut vinegar and its potential to remove aqueous calcium ions: column and batch studies. Environ Eng Res 28(1):210522–0. https://doi.org/10.4491/eer.2021.522
38. Sheng X, Wang J, Cui Q, Zhang W, Zhu X (2022) A feasible biochar derived from biogas residue and its application in the efficient adsorption of tetracycline from an aqueous solution. Environ Res 207:112175. https://doi.org/10.1016/j.envres.2021.112175
39. Petrovič A, Cenčič Predikaka T, Vohl S, Hostnik G, Finšgar M, Čuček L (2024) Hydrothermal conversion of oilseed cakes into valuable products: influence of operating conditions and whey as an alternative process liquid on product properties and their utilization. Energy Convers Manage 313:118640. https://doi.org/10.1016/j.enconman.2024.118640
40. Islam MA, Parvin MI, Dada TK, Kumar R, Antunes E (2024) Silver adsorption on biochar produced from spent coffee grounds: validation by kinetic and isothermal modelling. Biomass Convers Biorefin 14:28007–28021. https://doi.org/10.1007/s13399-022-03491-0
41. Liu Y, Cao Y, Yu Q (2022) In-situ deep eutectic solvent enhance hydrothermal carbonization of garden waste for methylene blue removal. Biomass Bioenergy 167:106626. https://doi.org/10.1016/j.biombioe.2022.106626
42. Fan J, Li Y, Yu H, Li Y, Yuan Q, Xiao H, Li F, Pan B (2020) Using sewage sludge with high ash content for biochar production and Cu(II) sorption. Sci Total Environ 713:136663. https://doi.org/10.1016/j.scitotenv.2020.136663
43. Lima ÉC, Adebayo MA, Machado FM (2015) Kinetic and Equilibrium Models of Adsorption. In: Bergmann CP, Machado FM (eds) Carbon Nanomaterials as Adsorbents for Environmental and Biological Applications. Springer International Publishing, Cham, pp 33–69
44. Huang H, Tang J, Gao K, He R, Zhao H, Werner D (2017) Characterization of KOH modified biochars from different pyrolysis temperatures and enhanced adsorption of antibiotics. RSC Adv 7(24):14640–14648. https://doi.org/10.1039/C6RA27881G
45. Fan M, Shao Y, Wang Y, Sun J, He H, Guo Y, Zhang S, Wang S, Li B, Hu X (2025) Evolution of pore structure and functionalities of activated carbon and phosphorous species in activation of cellulose with H3PO4. Renew Energy 240:122151. https://doi.org/10.1016/j.renene.2024.122151
46. Wang J, Wang S (2019) Preparation, modification and environmental application of biochar: a review. J Clean Prod 227:1002–1022. https://doi.org/10.1016/j.jclepro.2019.04.282
47. Tu R, Sun Y, Wu Y, Fan X, cheng S, Jiang E, Xu X (2022) The fuel properties and adsorption capacities of torrefied camellia shell obtained via different steam-torrefaction reactors. Energy 238:121969. https://doi.org/10.1016/j.energy.2021.121969
48. Sun L, Chen D, Wan S, Yu Z (2015) Performance, kinetics, and equilibrium of methylene blue adsorption on biochar derived from eucalyptus saw dust modified with citric, tartaric, and acetic acids. Bioresour Technol 198:300–308. https://doi.org/10.1016/j.biortech.2015.09.026
49. Ramón-Gonçalves M, Alcaraz L, Pérez-Ferreras S, León-González ME, Rosales-Conrado N, López FA (2019) Extraction of polyphenols and synthesis of new activated carbon from spent coffee grounds. Sci Rep 9(1):17706. https://doi.org/10.1038/s41598-019-54205-y
50. Mamaní A, Ramírez N, Deiana C, Giménez M, Sardella F (2019) Highly microporous sorbents from lignocellulosic biomass: different activation routes and their application to dyes adsorption. J Environ Chem Eng 7(5):103148. https://doi.org/10.1016/j.jece.2019.103148
51. Lonappan L, Liu Y, Rouissi T, Brar SK, Surampalli RY (2020) Development of biochar-based green functional materials using organic acids for environmental applications. J Clean Prod 244:118841. https://doi.org/10.1016/j.jclepro.2019.118841
52. Phan KA, Phihusut D, Tuntiwiwattanapun N (2022) Preparation of rice husk hydrochar as an atrazine adsorbent: optimization, characterization, and adsorption mechanisms. J Environ Chem Eng 10(3):107575. https://doi.org/10.1016/j.jece.2022.107575
53. Alatalo S-M, Repo E, Mäkilä E, Salonen J, Vakkilainen E, Sillanpää M (2013) Adsorption behavior of hydrothermally treated municipal sludge & pulp and paper industry sludge. Bioresour Technol 147:71–76. https://doi.org/10.1016/j.biortech.2013.08.034
54. Kasera N, Augoustides V, Kolar P, Hall SG, Vicente B (2022) Effect of surface modification by oxygen-enriched chemicals on the surface properties of pine bark biochars. Processes 10(10):2136. https://doi.org/10.3390/pr10102136
55. Wongrod S, Simon S, Guibaud G, Lens PNL, Pechaud Y, Huguenot D, van Hullebusch ED (2018) Lead sorption by biochar produced from digestates: consequences of chemical modification and washing. J Environ Manage 219:277–284. https://doi.org/10.1016/j.jenvman.2018.04.108
56. Zhang Z, Li Y, Ding L, Yu J, Zhou Q, Kong Y, Ma J (2021) Novel sodium bicarbonate activation of cassava ethanol sludge derived biochar for removing tetracycline from aqueous solution: performance assessment and mechanism insight. Bioresour Technol 330:124949. https://doi.org/10.1016/j.biortech.2021.124949
57. Li H-Z, Zhang Y-N, Guo J-Z, Lv J-Q, Huan W-W, Li B (2021) Preparation of hydrochar with high adsorption performance for methylene blue by co-hydrothermal carbonization of polyvinyl chloride and bamboo. Bioresour Technol 337:125442. https://doi.org/10.1016/j.biortech.2021.125442
58. Qiu B, Shao Q, Shi J, Yang C, Chu H (2022) Application of biochar for the adsorption of organic pollutants from wastewater: modification strategies, mechanisms and challenges. Sep Purif Technol 300:121925. https://doi.org/10.1016/j.seppur.2022.121925

59. Phuong DTM, Loc NX, Miyanishi T (2019) Efficiency of dye adsorption by biochars produced from residues of two rice varieties, Japanese Koshihikari and Vietnamese IR50404. Desalin Water Treat 165:333–351. https://doi.org/10.5004/dwt.2019.24496
60. Dao MU, Le HS, Hoang HY, Tran VA, Doan VD, Le TTN, Sirotkin A, Le VT (2021) Natural core-shell structure activated carbon beads derived from *Litsea glutinosa* seeds for removal of methylene blue: facile preparation, characterization, and adsorption properties. Environ Res 198:110481. https://doi.org/10.1016/j.envres.2020.110481
61. Zhang C, Meng L, Fang Z, Xu Y, Zhou Y, Guo H, Wang J, Zhao X, Zang S, Shen H (2024) Experimental and theoretical studies on the adsorption of bromocresol green from aqueous solution using cucumber straw biochar. Molecules 29(19):4517. https://doi.org/10.3390/molecules29194517
62. Yang C, Wu H, Cai M, Li Y, Guo C, Han Y, Zhang Y, Song B (2023) Valorization of food waste digestate to ash and biochar composites for high performance adsorption of methylene blue. J Clean Prod 397:136612. https://doi.org/10.1016/j.jclepro.2023.136612
63. Kousar S, Fan M, Javed K, Rashid M, Zhang S, Hu X (2024) Hydrothermal carbonization of fruit peels of varied origin forms hydrochar of distinct capability for adsorption of methylene blue. J Water Process Eng 65:105799. https://doi.org/10.1016/j.jwpe.2024.105799
64. Yang HI, Lou K, Rajapaksha AU, Ok YS, Anyia AO, Chang SX (2018) Adsorption of ammonium in aqueous solutions by pine sawdust and wheat straw biochars. Environ Sci Pollut Res 25(26):25638–25647. https://doi.org/10.1007/s11356-017-8551-2
65. Zhu G, Xing X, Wang J, Zhang X (2017) Effect of acid and hydrothermal treatments on the dye adsorption properties of biomass-derived activated carbon. J Mater Sci 52(13):7664–7676. https://doi.org/10.1007/s10853-017-1055-0
66. Xu Y, Liu Y, Liu S, Tan X, Zeng G, Zeng W, Ding Y, Cao W, Zheng B (2016) Enhanced adsorption of methylene blue by citric acid modification of biochar derived from water hyacinth (*Eichornia crassipes*). Environ Sci Pollut Res 23(23):23606–23618. https://doi.org/10.1007/s11356-016-7572-6
67. Liu Y, Ma S, Chen J (2018) A novel pyro-hydrochar via sequential carbonization of biomass waste: preparation, characterization and adsorption capacity. J Clean Prod 176:187–195. https://doi.org/10.1016/j.jclepro.2017.12.090
68. Zhang X, Gao B, Fang J, Zou W, Dong L, Cao C, Zhang J, Li Y, Wang H (2019) Chemically activated hydrochar as an effective adsorbent for volatile organic compounds (VOCs). Chemosphere 218:680–686. https://doi.org/10.1016/j.chemosphere.2018.11.144
69. Kimbi Yaah VB, Zbair M, de Botelho Oliveira S, Ojala S (2021) Hydrochar-derived adsorbent for the removal of diclofenac from aqueous solution. Nanotechnol Environ Eng 6(1):3. https://doi.org/10.1007/s41204-020-00099-5
70. Ding K, Zhou X, Hadiatullah H, Lu Y, Zhao G, Jia S, Zhang R, Yao Y (2021) Removal performance and mechanisms of toxic hexavalent chromium (Cr(VI)) with ZnCl<Subscript>2</Subscript> enhanced acidic vinegar residue biochar. J Hazard Mater 420:126551. https://doi.org/10.1016/j.jhazmat.2021.126551
71. Maged A, Elgarahy AM, Hlawitschka MW, Haneklaus NH, Gupta AK, Bhatnagar A (2023) Synergistic mechanisms for the superior sorptive removal of aquatic pollutants via functionalized biochar-clay composite. Bioresour Technol 387:129593. https://doi.org/10.1016/j.biortech.2023.129593
72. Satyam S, Patra S (2024) Innovations and challenges in adsorption-based wastewater remediation: a comprehensive review. Heliyon 10(9):e29573. https://doi.org/10.1016/j.heliyon.2024.e29573
73. Saba B, Christy AD, Shah A (2024) Hydrochar for pollution remediation: effect of process parameters, adsorption modeling, life cycle assessment and techno-economic evaluation. Resour Conserv Recycl 202:107359. https://doi.org/10.1016/j.resconrec.2023.107359
74. Alsawy T, Rashad E, El-Qelish M, Mohammed RH (2022) A comprehensive review on the chemical regeneration of biochar adsorbent for sustainable wastewater treatment. Npj Clean Water 5(1):29. https://doi.org/10.1038/s41545-022-00172-3
75. Ding H, Tong G, Sun J, Ouyang J, Zhu F, Zhou Z, Zhou N, Zhong M (2023) Regeneration of methylene blue-saturated biochar by synergistic effect of H2O2 desorption and peroxymonosulfate degradation. Chemosphere 316:137766. https://doi.org/10.1016/j.chemosphere.2023.137766